(8) Edwards, S. F. *Polym. Prepr. (Am. Chem. Soc., Div. Polym. Chem.)* 1981, *22*, 182.

(9) Vettegren, V. I.; Kusov, A. A.; Korzhavin, L. N.; Frenkel, S. Ya. *Polym. Sci. U.S.S.R. (Engl. Transl.)* 1982, *24*, 2241.

(10) Eyring, H. *J. Chem. Phys.* 1936, *4*, 283.

(11) Kauzmann, W.; Eyring, H. *J. Am. Chem. Soc.* 1940, *62*, 3113.

(12) Lazurkin, Yu. S.; Fogelson, R. A. *Zh. Tekh. Fiz.* 1951, *21*, 267.

(13) Lazurkin, Yu. S. *J. Polym. Sci.* 1958, *30*, 595.

(14) Zhurkov, S. N. *Int. J. Fract. Mech.* 1965, *1*, 311.

(15) Bartenev, G. M.; Zuyev, Yu. S. "Strength and Failure of Visco-Elastic Materials"; Pergamon: Oxford, 1968.

(16) Skolnick, J.; Perchak, D.; Yaris, R.; Schaefer, J. *Macromolecules* 1984, *17*, 2332.

(17) Robertson, R. E. *J. Chem. Phys.* 1966, *44*, 3950.

(18) Ferry, J. D. "Viscoelastic Properties of Polymers"; Wiley: New York, 1980; Chapters 15, 16, 18, 19.

(19) Aharoni, S. M. *J. Appl. Polym. Sci.* 1972, *16*, 3275.

(20) Aharoni, S. M. *J. Polym. Sci., Polym. Symp.* 1973, *No. 42*, 795.

(21) Aharoni, S. M. *J. Macromol. Sci., Phys.* 1974, *B9*, 699.

(22) Aharoni, S. M. In "Toughness and Brittleness of Plastics"; Deanin, R. D., Crugnola, A. M., Eds.; American Chemical Society: Washington, D. C., 1976; Adv. Chem. Ser. No. 154, pp 123–132.

(23) Aharoni, S. M. *J. Polym. Sci., Polym. Lett. Ed.* 1974, *12*, 549.

(24) Aharoni, S. M. *J. Appl. Polym. Sci.* 1977, *21*, 1323.

(25) Aharoni, S. M. *Macromolecules* 1983, *16*, 1722.

(26) Tobolsky, A.; Eyring, H. *J. Chem. Phys.* 1943, *11*, 125.

(27) Bueche, F. *J. Appl. Phys.* 1957, *28*, 784.

(28) Kramer, E. J. *J. Appl. Polym. Sci.* 1970, *14*, 2825.

(29) Kramer, E. J. *J. Appl. Phys.* 1970, *41*, 4327.

(30) Boyer, R. F. *Rubber Chem. Technol.* 1963, *36*, 1303.

(31) Graessley, W. W.; Edwards, S. F. *Polymer* 1981, *22*, 1329.

(32) Vincent, P. I. *Polymer* 1972, *13*, 558.

(33) Heijboer, J. *J. Polym. Sci., Part C* 1968, *16*, 3755.

(34) Nunes, R. W.; Martin, J. R.; Johnson, J. F. *Polym. Eng. Sci.* 1982, *22*, 205.

(35) Michel, J.; Manson, J. A.; Hertzberg, R. W. *Polymer* 1984, *25*, 1657.

# Effects of Polydispersity on the Linear Viscoelastic Properties of Entangled Polymers. 1. Experimental Observations for Binary Mixtures of Linear Polybutadiene

## Mark J. Struglinski[1a] and William W. Graessley*[1b]

*Chemical Engineering Department, Northwestern University, Evanston, Illinois 60201. Received April 29, 1985*

ABSTRACT: Viscoelastic effects of polydispersity for linear polymers in the entanglement regime were studied with binary mixtures of nearly monodisperse polybutadiene. Five series of mixtures (7–10 compositions in each) were investigated for component molecular weight ratios, $R = M_L/M_S$, from 2.5 to 10.7. Storage and loss moduli, $G'(\omega)$ and $G''(\omega)$, were measured for each composition over a wide range of frequencies at several temperatures and reduced to master curves at 25 °C. Viscosity $\eta_0$ and recoverable compliance $J_e^\circ$ were obtained and compared with a variety of proposed mixing laws. The peaks in $G''(\omega)$ were used to estimate relaxation times and weighting factors for the individual component contributions. The compositional dependence of these quantities was in fairly good agreement with the tube model and constraint lifetime ideas applied to mixtures.

## Introduction

The viscoelastic properties of polymer melts and solutions are strongly influenced by molecular weight distribution. In dilute solutions the effect of polydispersity is straightforward. If the chains do not interact, the polymeric contribution to stress is obtained by simple addition. In concentrated solutions and melts the chains overlap extensively; if they are long enough the behavior is dominated by entanglement interactions. How polydispersity affects linear viscoelastic behavior in such strongly interacting systems is a subject of longstanding interest.[2]

The shear stress relaxation modulus $G(t)$ contains all information on the linear viscoelastic behavior of a liquid and is a convenient property for discussion purposes. The dynamic shear modulus $G^*(\omega) = G'(\omega) + iG''(\omega)$ is more commonly measured and is related to $G(t)$ by Fourier transformation:

$$G^*(\omega) = i\omega \int_0^\infty G(t) \exp(-i\omega t) \, dt \qquad (1)$$

The values of steady-state viscosity at zero shear rate $\eta_0$ and steady-state recoverable shear compliance $J_e^\circ$ can be obtained from the moments of $G(t)$ or from the storage modulus $G'(\omega)$ and loss modulus $G''(\omega)$ at low frequencies:

$$\eta_0 = \int_0^\infty G(t) \, dt = \lim_{\omega \to 0} \frac{G''(\omega)}{\omega} \qquad (2)$$

$$J_e^\circ = \frac{1}{\eta_0^2} \int_0^\infty t G(t) \, dt = \lim_{\omega \to 0} \frac{G'(\omega)}{|G^*(\omega)|^2} \qquad (3)$$

The relaxation spectrum $H(\tau)$ is an equivalent expression of linear response which can be derived from data on $G(t)$ or $G^*(\omega)$ by an integral inversion, e.g.

$$G^*(\omega) = \int_{-\infty}^\infty \frac{i\omega\tau}{1 + i\omega\tau} H(\tau) \, d\ln\tau \qquad (4)$$

Extensive measurements have been made on highly entangled systems of nearly monodispersed linear chains. The response at long times or low frequencies is found to assume a universal form.[2-4] Thus, in the plateau and terminal regions

$$G(t) = G_N^\circ U(t/\tau_0) \qquad (5)$$

where $U(t/\tau_0)$ is a universal function, normalized to give $U(0) = 1$, $G_N^\circ$ is the plateau modulus, and $\tau_0$ is a characteristic time:

$$\tau_0 = \eta_0 J_e^\circ \qquad (6)$$

The terminal spectrum is quite narrow, and this, together with its large separation from the transition region for long chains ($M \gg M_e$), results in a prominent and well-defined peak in the loss modulus, $G_m''$ at $\omega_m$, and a rapid approach of $G'(\omega)$ to $G_N^\circ$ beyond $\omega_m$. The dimensionless products

$\omega_m \tau_0 \sim 2$ and $J_e{}^\circ G_N{}^\circ \sim 2.3$ appear to be universal constants for highly entangled linear polymers with narrow molecular weight distribution.[4-6]

Viscosity is proportional to $M^{3.4}$ for molecular weights greater than $M_c \sim 2M_e$. Recoverable compliance is independent of $M$ beyond $M_c{}' \sim 3M_c$; below $M_c{}'$ the values are in reasonable agreement with the modified Rouse model expression[2]

$$J_e{}^\circ = \frac{2}{5} \frac{M}{c R_G T} \qquad (7)$$

where $c$ is the polymer concentration (weight/volume), $R_G$ is the universal gas constant, and $T$ is the temperature. The entanglement molecular weight $M_e$ is defined in terms of the plateau modulus[2]

$$M_e \equiv c R_G T / G_N{}^\circ \qquad (8)$$

and $M/M_e$ is the entanglement density. When $M \gg M_e$, both $G_N{}^\circ$ and $J_e{}^\circ$ change with dilution according to power laws:

$$G_N{}^\circ \propto c^d \qquad (9)$$

$$J_e{}^\circ \propto c^{-d} \qquad (10)$$

with $2.0 < d < 2.3$ for many polymers and diluents.[2,4,7]

The effect of polydispersity for entangled linear chains has been studied extensively with binary mixtures of nearly monodisperse components.[2,8-15] The following features seem clearly established.

(a) Viscosity depends primarily on the weight-average molecular weight. Thus, for pure components and mixtures

$$\eta_0 = K \bar{M}_w{}^\alpha \qquad (11)$$

where $\alpha \sim 3.4$,[2]

$$\bar{M}_w = \phi_L M_L + \phi_S M_S \qquad (12)$$

and the $\phi$'s and $M$'s are volume fractions (equal to weight fractions) and molecular weights of the long-chain (L) and short-chain (S) components.

(b) Recoverable compliance is very sensitive to polydispersity. The value of $J_e{}^\circ$ rises steeply as small amounts of L chains are added to an S-chain matrix, passes through a maximum, $(J_e{}^\circ)_{max}$ at $(\phi_L)_{max}$, while $L$ is still the minority component ($\phi_L < \phi_S$), and finally approaches $(J_e{}^\circ)_L$ along the power law for simple dilution (eq 10)

$$J_e{}^\circ = (J_e{}^\circ)_L \phi_L{}^{-d} \qquad (13)$$

The values of $(J_e{}^\circ)_{max}$ become larger and $(\phi_L)_{max}$ becomes smaller as the ratio of component molecular weights, $R = M_L/M_S$, increases.

(c) Contributions of the individual components can be observed rather directly in $G^*(\omega)$ when both are entangled and $R$ is significantly larger than unity. Two peaks appear in $G''(\omega)$; the low-frequency peak $(G_m{}'')_L$ increases and the high-frequency peak $(G_m{}'')_S$ decreases with increasing $\phi_L$. The storage modulus $G'(\omega)$ has a corresponding inflection between $(\omega_m)_L$ and $(\omega_m)_S$. If the S component is well entangled ($M_S \gg M_e$), $G'(\omega)$ approaches the pure component plateau modulus between $(\omega_m)_S$ and the transition region, demonstrating that $G_N{}^\circ$ is independent of polydispersity.

A variety of generalizations about polydispersity effects have been proposed. Some of these take the form of empirical mixing laws, using simple combinations of the component spectra. Weighting factors, time scale shifts, and cross-term forms are chosen to force agreement with such features as $\eta_0 \propto \bar{M}_w{}^{3.4}$ and constancy of $G_N{}^\circ$.[17,22-26]

Others are motivated by molecular arguments,[27,28] modified with adjustable parameters,[29] alternative forms for the weighting factors,[19,30] or generalized to incorporate competing mechanisms.[20,31] Still others focus on polydispersity effects in $\eta_0$ or $J_e{}^\circ$ alone.[15,32-34] Some of these proposals are clearly incompatible with observations on entangled mixtures,[2,3] but even the more promising approaches have been tested for only limited ranges of $R$ and $M_S/M_e$.

This paper reports experimental results on $G^*(\omega)$ for several series of highly entangled binary mixtures of linear polybutadiene. Like polystyrene, upon which most recent studies are based, polybutadiene can be synthesized with high molecular weight and narrow distribution by anionic polymerization. Polybutadiene has certain advantages, however, which are related to both its low $T_g \sim -97$ °C and small $M_e = 1850$, compared with $T_g \sim 100$ °C and $M_e = 18\,000$ for polystyrene. Measurements can be made in the vicinity of room temperature for polybutadiene even in highly entangled mixtures ($M_S/M_e \gg 1$) with moderate to large values of $R$. Elevated temperatures are required for polystyrene, and thermal degradation precludes measurements for ranges of $M_S/M_e$ and $R$ which are rather easily attained with polybutadiene. To gain these advantages, polybutadiene must be stabilized against oxidation, and care must be taken to minimize variations in chemical microstructure (cis-1,4, trans-1,4, and 1,2 vinyl enchainment) among the samples.

Five series of mixtures have been investigated, four in the undiluted state and one at 50 wt % of polymer. In all cases $M_S/M_e$ is larger than 20. The ratio of component molecular weights ranges from $R = 2.5$ to $R = 10.7$. For three series this ratio is approximately the same ($R \sim 4.5$) but achieved with different values of $M_S$ and $M_e$. Some results on polybutadiene mixtures have already been reported[15,16] and a few data are available with low molecular weight polybutadiene as the diluent.[4,35] Changes in component contributions to $G^*(\omega)$ with mixture composition are discussed here, and $\eta_0(\phi_L,R)$ and $J_e{}^\circ(\phi_L,R)$ are compared with calculations based on some proposed mixing laws. A second paper will follow, comparing $\eta_0$ and $J_e{}^\circ$ behavior with predictions based on the Doi–Edwards tube model[18] as modified to include the effect of tube constraint lifetimes.[31,36-38] A third paper will present a detailed molecular theory for the frequency dependence.[39] A fourth paper will report the experimental results for several series of linear–star and star–star mixtures.[40]

## Experimental Procedures

**1. Molecular Characterization.** Several samples of narrow-distribution polybutadiene were prepared by anionic polymerization in cyclohexane at 50 °C. Polymerization was initiated by *sec*-butyllithium and terminated by the addition of dry 2-propanol. The polymers were precipitated with methanol, stabilized, dried, and stored as described previously.[6,41]

Chemical microstructure of the polymers, determined by infrared spectroscopy,[6] is reported in Table I. With increasing chain length the cis-1,4 content decreases, the trans-1,4 content increases, and there is a small decrease in 1,2 (vinyl) content. These trends are consistent with earlier data for polybutadienes prepared by a similar method.[6] They appear to have little effect on rheological properties, although the slightly larger temperature coefficient and slightly smaller plateau modulus of sample 41L (see below) may be related to such differences. For this limited range of microstructures and molecular weights the density of polybutadiene at 25 °C is 0.895 g/cm³ and the glass transition temperature is -97 °C.[6,41]

Molecular weight distributions were estimated by gel permeation chromatography (Waters Associates, Model 200) in tetrahydrofuran at room temperature.[5] Values of $\bar{M}_w/\bar{M}_n$, corrected for axial dispersion, are given in Table I. No sample was used in the rheological work unless its chromatogram was sym-

### Table I
### Molecular Characterization Data on the Component Polybutadienes

| sample | % 1,4 cis | % 1,4 trans | % 1,2 | [$\eta$](THF), dL/g | $M$(IV)$^a$ | $M$(LS) | $\bar{M}_w/\bar{M}_n$(GPC) |
|---|---|---|---|---|---|---|---|
| 41L | 42 | 50 | 8 | 0.65 | 40 700 | 39 000 | 1.04 |
| 98L | 47 | 45 | 8 | 2.36 | 97 500 | 92 500 | 1.03 |
| 174L | 50 | 43 | 7 | 1.93 | 174 000 | 181 000 | 1.04 |
| 435L | 58 | 36 | 6 | 3.84 | 435 000 | 450 000 | 1.03 |

$^a$ Calculated from intrinsic viscosity in tetrahydrofuran with eq 12.

### Table II
### Characteristics of the Mixtures Investigated

| series | $\phi_p{}^a$ | $R^b$ | $M_e{}^c$ | range of $\bar{M}_w/\bar{M}_e{}^d$ |
|---|---|---|---|---|
| 174L/435L | 1.0 | 2.5 | 1850 | 98–243 |
| 98L/435L | 1.0 | 4.5 | 1850 | 50–243 |
| 98L/435L(soln) | 0.52 | 4.5 | 4400 | 21–103 |
| 41L/174L | 1.0 | 4.3 | 1850 | 21–98 |
| 41L/435L | 1.0 | 10.7 | 1850 | 21–243 |

$^a$ Volume fraction of total polymer in the series. $^b$ Ratio of molecular weights of long-chain (L) and short-chain (S) components: $R = M_L/M_S$. $^c$ Calculated with eq 8. $^d$ $\bar{M}_w$ values calculated with eq 12 using $M$(IV) for the components.

metrical, free of high and low molecular weight tails, and gave a value of $\bar{M}_w/\bar{M}_n$ less than 1.05. Candidate samples were further screened on the basis of their rheological properties, as described below.

Molecular weights were obtained from intrinsic viscosity measurements and dilute solution light scattering. Values of $M$ were calculated from [$\eta$], measured in tetrahydrofuran at 25 °C, using

$$[\eta] = 2.27 \times 10^{-4} M^{0.75} \qquad (14)$$

This equation was established earlier with other samples of similar microstructure[41] and confirmed more recently by other workers.[42] The light scattering measurements was made in cyclohexane at 25 °C (Chromatix KMX-6, $\lambda$ = 632.8 nm). Molecular weights were calculated with $dn/dc$ = 0.110$_5$ mL/g, a value determined earlier for similar polybutadienes.[6]

The data in Table I demonstrate fairly good agreement between the two methods. We have used the molecular weights from intrinsic viscosity in subsequent tables and figures only because we regard them as slightly more accurate in relative values. That choice does not affect the conclusions in any significant way. The component polybutadienes are identified according to molecular weight; e.g., 98L is the sample with $M$ = 97 700, as calculated from [$\eta$] with eq 14.

**2. Preparation of Mixtures.** The polymer mixtures, 7–10 compositions for each series, were prepared by dissolving weighed amounts of the individual components in a large excess of benzene. The benzene mixtures were kept in the dark and stirred gently until complete dissolution ($\sim$24 h). The benzene was then evaporated and the samples dried at least 1 week in a vacuum oven at room temperature. Solvent removal was considered to be complete when the change in weight on successive days was less than 0.01%. One series of mixtures was diluted 50% by weight with Flexon 391 (Exxon Chemical Co.), a naphthenic hydrocarbon oil of low volatility with $\eta_s$ = 43.3 P and $\rho$ = 0.979 g/cm$^3$ at 25 °C.[4,35] Benzene was again used to assist dissolution and then removed as before. The volume fraction of polymer in

this series was 0.52, calculated from the component densities with the assumption of no volume change upon mixing. The general characteristics of the five series are summarized in Table II.

**3. Rheological Measurements.** Storage and loss moduli were determined by the eccentric rotating disk (ERD) method with a Rheometrics mechanical spectrometer. Parallel plates 25 mm in diameter were used with a typical gap spacing of 1.2 mm. The samples were blanketed with nitrogen, and measurements were made at several temperatures (25, 50, 75, and, in a few cases, near 0 °C). The full range of the instrument, $10^{-3} < \omega < 100$ rad/s, was used wherever possible. The strain amplitude was varied somewhat over this range, depending on the magnitude of the forces. Small strains ($\gamma \sim 0.05$) were always used when $|G^*|$ was large, but in no case were the strain amplitudes larger than $\gamma$ = 0.3. Linearity of response was checked repeatedly; all data reported here were obtained well within the linear region.

Values of $G'(\omega)$ and $G''(\omega)$ were calculated from steady-state forces and the strain, corrected for instrumental compliance. Compliance corrections are necessary for $G'(\omega)$ at low frequencies, where $G'(\omega) \ll G''(\omega)$, and become important for both $G'(\omega)$ and $G''(\omega)$ when $|G^*(\omega)|$ exceeds $\sim 5 \times 10^6$ dyn/cm$^2$. For the pure component polybutadienes the latter range is reached just beyond the terminal loss peak in $G''(\omega)$. As $|G^*(\omega)|$ approaches $10^7$ dyn/cm$^2$ the corrected values of the moduli, and especially of $G''(\omega)$, become very sensitive to the choice of $K_I$, the radial compliance of the instrument. The value used here for all the data, $K_I = 4.35 \times 10^{-9}$ cm/dyn, was carefully estimated from measurements at different gap settings and modulus magnitudes.[40] That value, however, may not be precisely correct for the undiluted 98L/435L series. Those data had been gathered early in the work, prior to a mechanical modification of the instrument that may have changed the stiffness slightly. The value of $K_I$ given above and the data for all other series were measured after the modification. We believe this small uncertainty in $K_I$ is responsible for the apparent anomalies at high frequencies, noted below, in the undiluted 98L/435L series. The diluted 98L/435L series should be the least affected by instrumental compliance because the plateau modulus, and therefore $|G^*(\omega)|$ at high frequencies, is much smaller for the solutions.

The data obtained at different temperatures were reduced to master curves at 25 °C. Excellent superposition was obtained by shifts in the frequency scale alone: no shift in modulus scale was necessary. The temperature–frequency shift factor $a_T$ is recorded for the pure components at 50 and 75 °C in Table III and at 50 °C for the mixtures in Table IV. Average values of $a_T$ = 0.36 at 50 °C, 0.17 at 75 °C, and $\sim$6.0 at −7 °C, are in reasonable agreement with measurements on other polybutadienes of the same microstructure.[2,40] Master curves for one of the pure components are shown in Figure 1 and for one series of mixtures in Figures 2 and 3.

**4. Evaluation of Rheological Parameters.** Values of $\eta_0$ were obtained from $G''(\omega)$ at low frequencies according to eq 2. Results

### Table III
### Rheological Properties of Pure Component Polybutadienes

| sample | $\eta_0$(25 °C), P | $a_T$(50 °C) | $a_T$(75 °C) | $10^{-6} G_m''$, dyn/cm$^2$ | $\omega_m$(25 °C), s$^{-1}$ | $10^{-7} G_N°$,$^a$ dyn/cm$^2$ | $10^7 J_e°$, cm$^2$/dyn | $J_e° G_N°$ |
|---|---|---|---|---|---|---|---|---|
| 41L | $1.3_5 \times 10^4$ | 0.39 | 0.19 | 2.95 | 500 | $1.0_5$ | 1.8 | 1.9 |
| 98L | $3.1 \times 10^5$ | 0.35 | 0.16 | $3.4_5$ | 32 | $1.2_5$ | $2.0_0$ | 2.5 |
| 98L(soln) | $6.9 \times 10^4$ | | | 0.76 | 35 | 0.27 | $9.3_3$ | 2.5 |
| 174L | $2.9_5 \times 10^6$ | 0.35 | 0.15 | $3.4_0$ | 4.0 | $1.2_0$ | 1.8 | 2.2 |
| 435L | $4.8 \times 10^7$ | 0.35 | 0.16 | $3.4_5$ | 0.25 | $1.2_5$ ($1.3_0$) | 2.1 | 2.6 |
| 435L(soln)$^b$ | $(1.0_5 \times 10^7)$ | | | | (0.25) | | | |

$^a$ Values obtained from $G_m''$ with eq 16; value in parentheses from eq 17. $^b$ Values estimated by extrapolation of results on the diluted 98L/435L series.
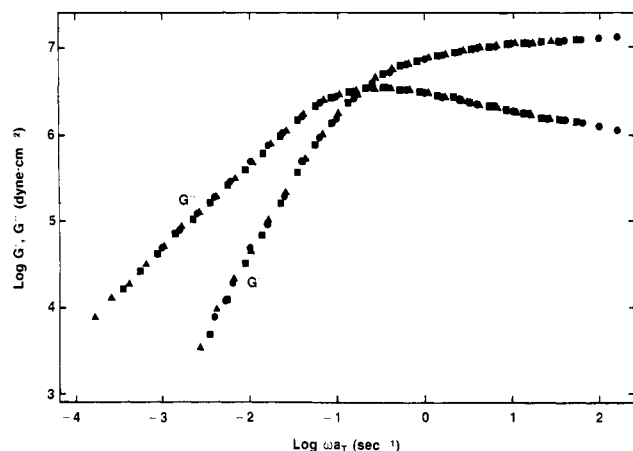
**Figure 1.** Dynamic shear modulus for pure component sample 435L. Data were obtained at 25 (●), 50 (■), and 75 °C (▲) and shifted along the frequency axis to form master curves at 25 °C.
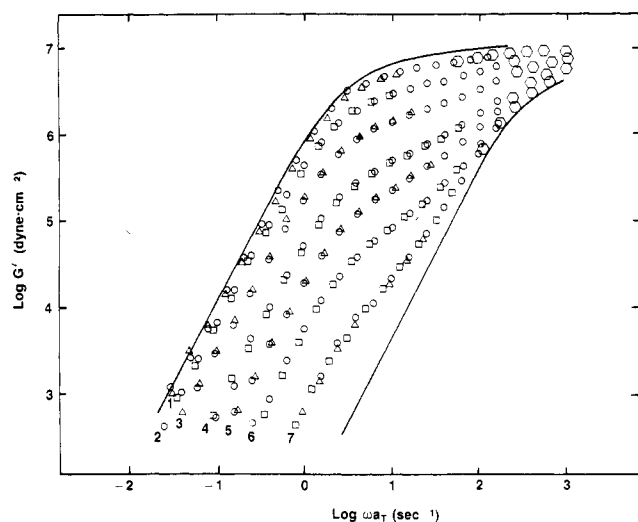


**Figure 2.** Storage modulus master curves at 25 °C for selected mixtures in the 41L/174L series. Master curves for the pure components are shown as solid lines. Mixture data were obtained at 25 (O), 50 (□), 75 (△), and near 0 °C (O) for $\phi_L$ = 0.90 (1), 0.70 (2), 0.50 (3), 0.30 (4), 0.20 (5), 0.10 (6), and 0.025 (7).
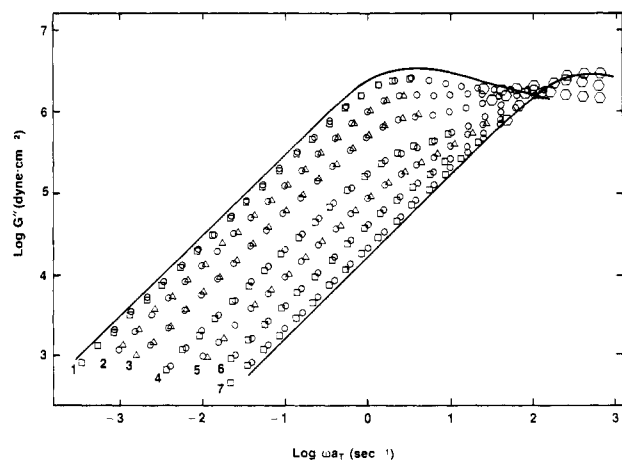


**Figure 3.** Loss modulus master curves at 25 °C for selected mixtures in the 41L/174L series. Mixture compositions are as given in Figure 2.

for the undiluted pure components at 25 °C (Table III) agree reasonably well with a correlation of the data for narrow-distribution polybutadiene (~8% vinyl) content reported by many investigators:[43]

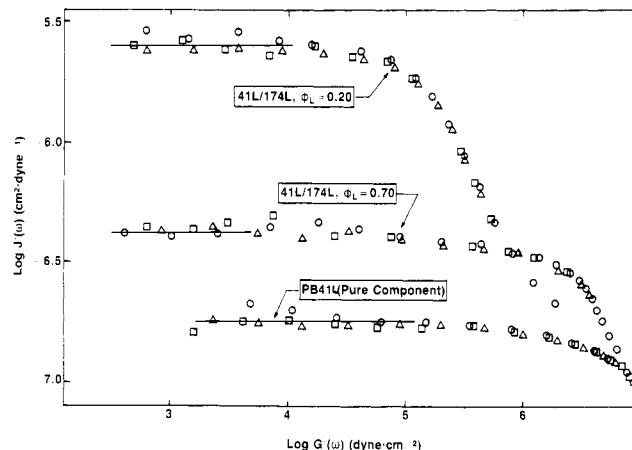$$\eta_0 = 3.63 \times 10^{-12}M^{3.41} \qquad (P) \qquad (15)$$



**Figure 4.** Storage compliance vs. storage modulus for a pure component and selected mixtures with large $\phi_L$. Symbols denote data obtained at 25 (O), 50 (□), and 75 °C (△).
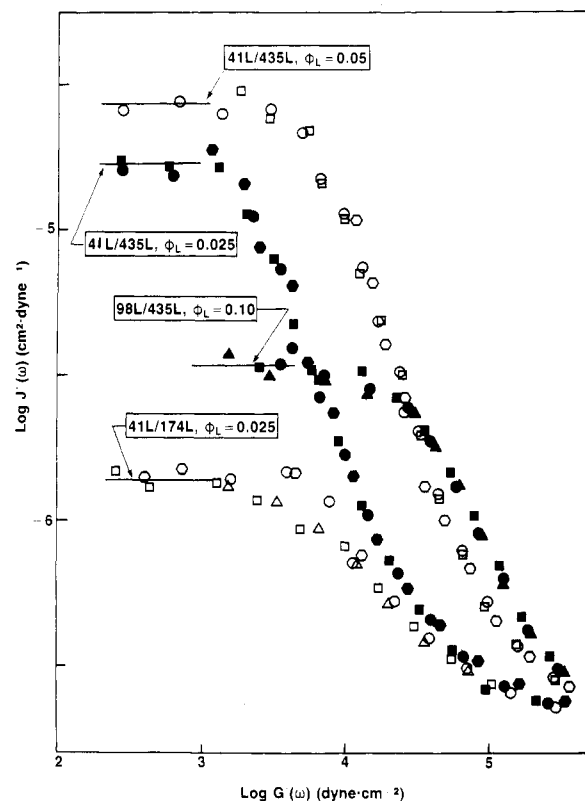


**Figure 5.** Storage compliance vs. storage modulus for selected mixtures with small $\phi_L$. Symbols denote data obtained at 0 (O), 25 (●, O), 50 (□, ■), and 75 °C, (△, ▲).

Values of $\eta_0$ for the mixtures are given in Table IV.

Values of $J_e{}^\circ$ were obtained from the storage compliance $J'(\omega)$ = $G'(\omega)/|G^*(\omega)|^2$ at low frequencies (eq 3). Storage compliance was plotted as a function of storage modulus, the result being a single curve for all temperatures because the temperature shift in modulus scale is negligible. Representative results are shown in Figures 4 and 5.

The behavior of $J'(\omega)$ is very sensitive to polydispersity,[14] and we found that to be useful as a final screen in the selection of pure components. Typical results for the nearly monodisperse pure components and mixtures with a high concentration of the L component are shown in Figure 4. In those cases $J'(\omega)$ settles into its low-frequency limit, $J_e{}^\circ$, while $G'(\omega)$ is still relatively large. A few pure component candidates were in fact rejected because $J'(\omega)$ continued to increase more or less indefinitely with decreasing $G'(\omega)$. Values of $J_e{}^\circ$ are given in Table III for the component polybutadienes. The average for the undiluted samples, $J_e{}^\circ$ = 1.9 × 10$^{-7}$ cm²/dyn, agrees well with earlier results on similar polybutadienes ($M > M_c'$ ~ 11 000$^4$).
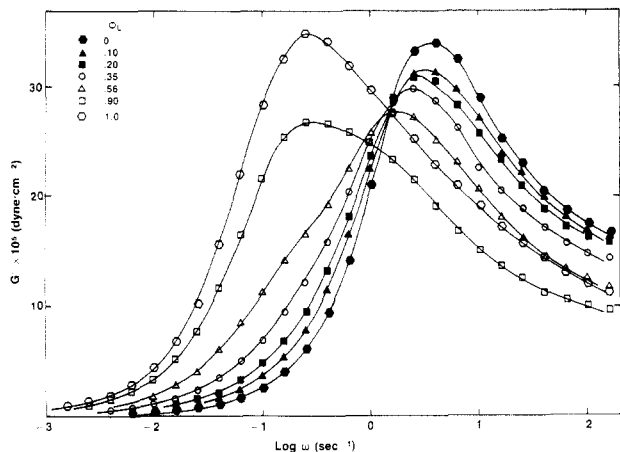
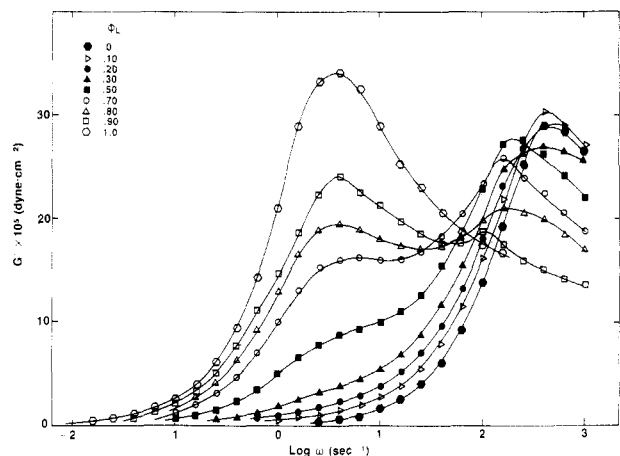**Figure 6.** Loss modulus master curves for selected 174L/435L mixtures at 25 °C.



**Figure 7.** Loss modulus master curves for selected 41L/174 L mixtures at 25 °C.



**Figure 8.** Loss modulus master curves for selected 98L/435L mixtures at 25 °C.



**Figure 9.** Loss modulus master curves for selected 41L/435L mixtures at 25 °C. The dashed curve is the trajectory of $(\omega)_L$ values expected for dilution by monomeric solvents as discussed later in the paper.



**Figure 10.** Loss modulus master curves for selected mixtures in the diluted 98L/435L solution series at 25 °C.

Values of $J_e{}^\circ$ were always more difficult to estimate for mixtures containing a small amount of the L component. Figure 5 shows $J'(\omega)$ vs. $G'(\omega)$ for several such mixtures. Limiting behavior was reached at much lower modulus levels, and the correspondingly small forces were difficult to measure accurately because of transducer sensitivity and drift. Data gathered at high temperatures were generally more reliable simply because the ERD forces reached steady state more quickly. Results for the mixtures are given in Table IV. We regard the reported values of $J_e{}^\circ$ for $\phi_L = 0.025$ as only reasonable estimates. For $0.05 \leq \phi_L \leq 0.15$ the uncertainty is perhaps 20%; for $\phi_L > 0.15$ and for the pure components the uncertainty is about 10%.

Plateau moduli for the components (Table III) were estimated from the loss modulus maximum:[4]

$$G_N{}^\circ = 3.56 G_m''\tag{16}$$

A value was also obtained for sample 435L by integrating the area under the loss peak after resolving out a slight overlap from the transition dispersion:[2,39]

$$G_N{}^\circ = \frac{2}{\pi} \int_{-\infty}^{\infty} G''(\omega)\, d \ln \omega\tag{17}$$

The average of values for the undiluted components, $G_N{}^\circ = 1.20 \times 10^7$ dyn/cm², agrees well with earlier results for this polybutadiene microstructure.[2,4,35,40] Values of $G'(\omega)$ for pure components and mixtures converge at high frequencies, confirming that $G_N{}^\circ$ is indeed independent of polydispersity. The ratio of loss peak maxima for undiluted 98L and its solution in Flexon 391, $(G_m'')_\text{soln}/(G_m'')_\text{melt} = 0.22$, agrees well with the value expected from an earlier study,[4] $(0.52)^{2.26} = 0.23$. The ratio of compliances, $(J_e{}^\circ)_\text{soln}/(J_e{}^\circ)_\text{melt} = 4.7$, compares reasonably well with the expected value of $(0.52)^{-2.24} = 4.3$, and so does $(\eta_3\omega_m)_\text{soln}/(\eta_0\omega_m)_\text{melt} = 0.24$,

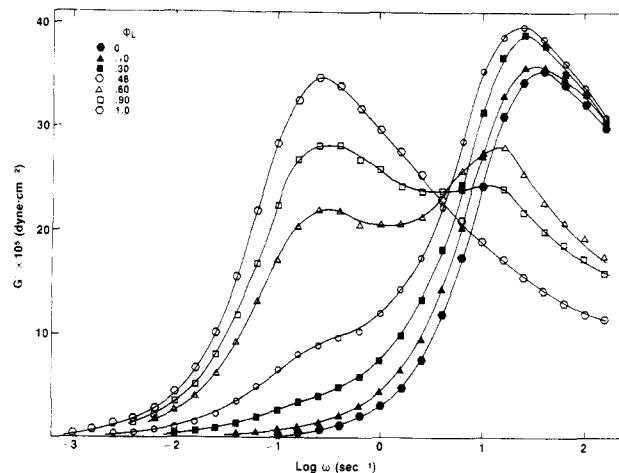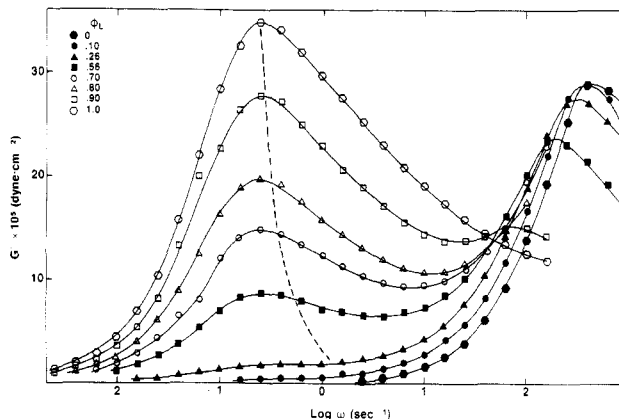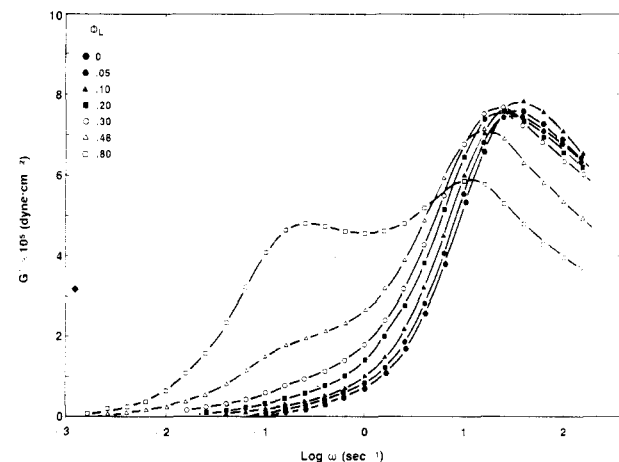compared with $(0.52)^{2.22} = 0.23$. The average of the product $J_e{}^\circ G_N{}^\circ$ is 2.33 for the pure components, also in line with other results.[4-6] From eq 8, $M_e = 1850$ for undiluted polybutadiene and $M_e = 4400$ for the diluted series.

## Results

**1. Observations on the Dynamic Modulus.** Some investigators have chosen to recast their results in terms of the relaxation spectrum. Such manipulation of the experimental data by numerical inversion of expressions

**Table IV**
**Viscoelastic Parameters**

(a) Series 174L/435L ($R$ = 2.5)

| $\phi_L$ | $\eta_0$(25 °C), P | $a_T$(50 °C) | $J_e{}^\circ$, cm$^2$/dyn | $(G_m{}'')_L$, dyn/cm$^2$ | $(\omega_m)_S$, s$^{-1}$ |
|---|---|---|---|---|---|
| 0.025 | $3.1 \times 10^6$ | 0.36 | $4.7 \times 10^{-7}$ | | 4.0 |
| 0.05 | $3.3_5 \times 10^6$ | 0.36 | $5.9 \times 10^{-7}$ | | 4.0 |
| 0.10 | $4.2 \times 10^6$ | 0.36 | $8.9 \times 10^{-7}$ | | 3.2 |
| 0.15 | $5.1 \times 10^6$ | $0.35_5$ | $10.5 \times 10^{-7}$ | | 3.2 |
| 0.20 | $6.4_5 \times 10^6$ | 0.35 | $8.7 \times 10^{-7}$ | | 2.8 |
| 0.35 | $1.0_5 \times 10^7$ | 0.40 | $6.8 \times 10^{-7}$ | | 2.5 |
| 0.56 | $1.7_5 \times 10^7$ | | $4.7 \times 10^{-7}$ | $1.6_5 \times 10^6$ | 1.6 |
| 0.90 | $3.6_5 \times 10^7$ | 0.37 | $2.8 \times 10^{-7}$ | $2.7 \times 10^6$ | |

(b) Series 98L/435L ($R$ = 4.5)

| $\phi_L$ | $\eta_0$(25 °C), P | $a_T$(50 °C) | $J_e{}^\circ$, cm$^2$/dyn | $(G_m{}'')_L$, dyn/cm$^2$ | $(\omega_m)_S$, s$^{-1}$ |
|---|---|---|---|---|---|
| 0.025 | $5.0 \times 10^5$ | 0.39 | $2.5 \times 10^{-6}$ | | 32 |
| 0.05 | $5.0 \times 10^5$ | 0.27 | $2.8 \times 10^{-6}$ | | 32 |
| 0.10 | $8.5 \times 10^5$ | 0.36 | $3.4 \times 10^{-6}$ | | 32 |
| 0.20 | $2.0_0 = 10^6$ | 0.35 | $2.2 \times 10^{-6}$ | $2.5 \times 10^5$ | 25 |
| 0.30 | $3.8 \times 10^6$ | 0.36 | $1.7 \times 10^{-6}$ | $4.0 \times 10^5$ | 25 |
| 0.48 | $9.7 \times 10^6$ | 0.36 | $7.8 \times 10^{-7}$ | $9.6 \times 10^5$ | 20 |
| 0.80 | $2.7_5 \times 10^7$ | 0.36 | $3.6 \times 10^{-7}$ | $2.2 \times 10^6$ | 14 |
| 0.90 | $3.4_5 \times 10^7$ | 0.36 | $2.8 \times 10^{-7}$ | $2.8_2 \times 10^6$ | 10 |

(c) Series 41L/174L ($R$ = 4.3)

| $\phi_L$ | $\eta_0$(25 °C), P | $a_T$(50 °C) | $J_e{}^\circ$, cm$^2$/dyn | $(G_m{}'')_L$, dyn/cm$^2$ | $(\omega_m)_S$, s$^{-1}$ |
|---|---|---|---|---|---|
| 0.025 | $2.1 \times 10^4$ | 0.35 | $1.4 \times 10^{-6}$ | | 500 |
| 0.05 | $2.6 \times 10^4$ | 0.34 | $2.5 \times 10^{-6}$ | | 500 |
| 0.10 | $4.4 \times 10^4$ | 0.36 | $3.1 \times 10^{-6}$ | | 500 |
| 0.15 | $6.6 \times 10^4$ | 0.35 | $2.9 \times 10^{-6}$ | | 360 |
| 0.20 | $1._0 \times 10^5$ | 0.35 | $2.5 \times 10^{-6}$ | | 400 |
| 0.30 | $2.0_0 \times 10^5$ | 0.36 | $1.5 \times 10^{-6}$ | $4.2 \times 10^5$ | 360 |
| 0.50 | $6.0 \times 10^5$ | 0.35 | $7.1 \times 10^{-7}$ | $8.9 \times 10^5$ | 225 |
| 0.70 | $1.3 \times 10^6$ | 0.36 | $4.2 \times 10^{-7}$ | $1.6 \times 10^6$ | 180 |
| 0.80 | $1.7 \times 10^6$ | 0.36 | $3.2 \times 10^{-7}$ | $2.0 \times 10^6$ | 170 |
| 0.90 | $2.3 \times 10^6$ | 0.35 | $2.3 \times 10^{-7}$ | $2.4 \times 10^6$ | 115 |

(d) Series 41L/435L ($R$ = 10.7)

| $\Phi_L$ | $\eta_0$(25 °C), P | $a_T$(50 °C) | $J_e{}^\circ$, cm$^2$/dyn | $(G_m{}'')_L$, dyn/cm$^2$ | $(\omega_m)_S$, s$^{-1}$ |
|---|---|---|---|---|---|
| 0.025 | $2.9 \times 10^4$ | 0.35 | $1.7_0 \times 10^{-5}$ | | 500 |
| 0.05 | $6.0 \times 10^4$ | 0.35 | $2.7 \times 10^{-5}$ | | 500 |
| 0.10 | $1.91 \times 10^5$ | 0.36 | $1.6 \times 10^{-5}$ | $4.2 \times 10^4$ | 400 |
| 0.15 | $4.0_5 \times 10^5$ | 0.39 | $9.8 \times 10^{-6}$ | $6.3 \times 10^4$ | 400 |
| 0.26 | $1.7_5 \times 10^6$ | 0.37 | $4.9 \times 10^{-6}$ | $1.8 \times 10^5$ | 360 |
| 0.36 | $3.7 \times 10^6$ | 0.36 | $2.4 \times 10^{-6}$ | $3.1_5 \times 10^5$ | |
| 0.56 | $1.0_0 \times 10^7$ | 0.37 | $8.7 \times 10^{-7}$ | $8.5 \times 10^5$ | 180 |
| 0.70 | $1.7_5 = 10^7$ | 0.38 | $5.0 \times 10^{-7}$ | $1.48 \times 10^6$ | |
| 0.80 | $2.3_5 \times 10^7$ | 0.34 | $3.7 \times 10^{-7}$ | $1.9_5 \times 10^6$ | |
| 0.90 | $3.4 \times 10^7$ | | $3.0 \times 10^{-7}$ | $2.7 \times 10^6$ | |

(e) 98L/435L Solution Series ($R$ = 4.5)

| $\phi_L$ | $\eta_0$(25 °C), P | $J_e{}^\circ$, cm$^2$/dyn | $(G_m{}'')_L$, dyn/cm$^2$ | $(\omega_m)_S$, s$^{-1}$ | $\eta_0/(\eta_0)^{\circ a}$ | $J_e{}^\circ/(J_e{}^\circ)^{\circ a}$ |
|---|---|---|---|---|---|---|
| 0.0 | $6.99 \times 10^4$ | $9.3_3 \times 10^{-7}$ | | 35 | 0.22 | 4.7 |
| 0.025 | $1.0 \times 10^5$ | $8.7 \times 10^{-6}$ | | 35 | 0.21 | 3.5 |
| 0.05 | $1.1_5 \times 10^5$ | $1.0 \times 10^{-5}$ | | 35 | 0.23 | 3.6 |
| 0.10 | $1.6_5 \times 10^5$ | $1.6 \times 10^{-5}$ | | 35 | 0.20 | 4.6 |
| 0.20 | $4.2_5 \times 10^5$ | $1.0_0 \times 10^{-5}$ | | 26 | 0.21 | 4.6 |
| 0.30 | $8.3 \times 10^5$ | $7.9_4 \times 10^{-6}$ | | 23 | 0.22 | 4.8 |
| 0.48 | $2.3_5 \times 10^6$ | $3.4 \times 10^{-6}$ | $(1.9 \times 10^5)$ | 21 | 0.24 | 4.4 |
| 0.80 | $6.9 \times 10^6$ | $1.7 \times 10^{-6}$ | $4.8 \times 10^5$ | 14 | 0.25 | 4.8 |

$^a$ $(\eta_0)^\circ$ and $(J_e{}^\circ)^\circ$ are the values for undiluted mixtures of the same polymer composition.

such as eq 4 is unnecessary in our judgment, and it also introduces some additional uncertainty, making the comparison among studies more prone to error. Plots of $G''(\omega)$ vs. log $\omega$ provide a rather direct and convenient alternative. Results in this form are shown in Figures 6–10 for the five series of mixtures.

The general character of such plots for a binary mixture of intermediate composition, showing terminal loss peaks for the L and S components and the tail of the loss peak from the transition region, is sketched in Figure 11. In principle, the transition contribution is independent of molecular weight when $M$ is large, and thus its contribution

to $G''(\omega)$ at each frequency should be independent of mixture composition. Furthermore, the area under the combined L and S terminal peaks depends only on the plateau modulus (eq 17) and thus should also be independent of mixture composition. For a linear mixing law the individual areas would be proportional to $\phi_L$ and $\phi_S$, respectively.[22]

Rather than attempt to resolve the individual peaks (the dashed lines in Figure 11), we have used simply the loss peak maxima, $(G_m{}'')_L$ and $(G_m{}'')_S$, and loss peak frequencies, $(\omega_m)_L$ and $(\omega_m)_S$, to characterize the effects of composition. Broadly speaking, the reciprocal of $\omega_m$ corre-
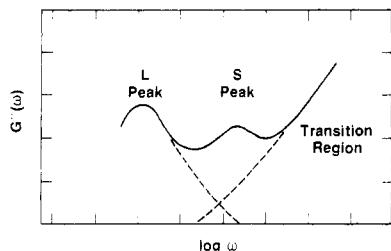
**Figure 11.** Schematic behavior of the loss modulus for a binary mixture of nearly monodisperse components.
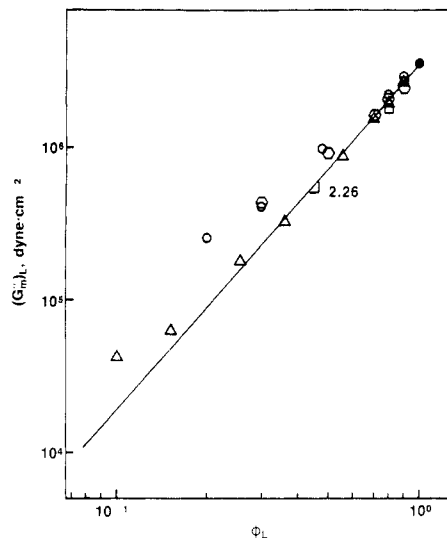


**Figure 12.** Compositional dependence of the loss modulus maximum for L chains in undiluted mixtures. Symbols denote values for the 41L/435L series (△), the 98L/435L series (O), the 174L/435L series (□), and the 41L/174L series (◇). The line indicates behavior for nearly monodisperse polybutadienes diluted by a monomeric solvent.[4]

sponds to a mean relaxation time. With $\tau_0$ defined by eq 6 we find

$$\omega_m^{-1} \sim 0.45\tau_0 \tag{18}$$

for the pure components (sample 41L has a somewhat larger numerical coefficient). Likewise, $G_m''$ corresponds to the weighting factor associated with the relaxation.

In interpreting changes in $G_m''$ and $\omega_m$ with mixture composition, however, it is necessary to bear in mind some possible complications. First, those values may be affected by peak overlap. This problem is less severe for the L peak, which has interference only on the high-frequency side. The S peak, sandwiched between the L peak and the transition region, has interference on both sides. Sensitivity to overlap can be gauged to some extent by comparing behavior for mixtures with different peak separations, i.e., different values of $R$ and $M_S/M_e$, but even this test is ambiguous because those compositional differences could, in themselves, influence the positions of even perfectly resolved peaks. Second, $\omega_m$ and $G_m''$ track the mean relaxation time and spectral weighting only if the *shape* of the loss peak does not change with composition. The effect of shape changes is considered in more detail below.

**A. Properties of the L Peak.** Values of $(G_m'')_L$ for the mixtures are recorded in Table IV. Figure 12 shows $(G_m'')_L$ vs. $\phi_L$ for the four undiluted series. The solid line is the behavior obtained for monomeric diluents, including an oligomeric polybutadiene with $M < M_c$: $G_m'' \propto \phi_L^{2.26}$.[4] Dilution with S chains gives the same behavior in the high-$\phi_L$ range even when $M_S \gg M_c$. Departure from this solvent-like dependence appears eventually in all series,
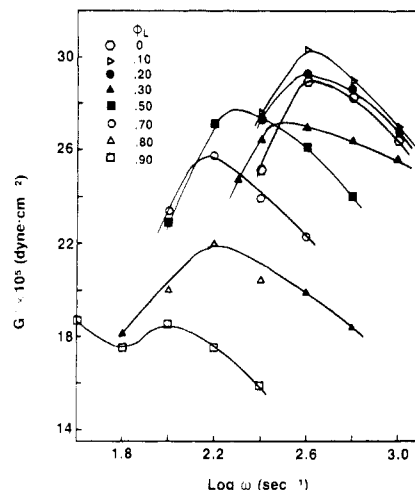


**Figure 13.** Expanded plot of loss modulus for mixtures of the 41L/174L series near the S peak.

and it appears at smaller $\phi_L$ for larger $R$. For $R = 10.7$ (the 41L/435L series) the $\phi_L^{2.26}$ behavior persists down to $\phi_L \sim 0.2$. For constant $R \sim 4.5$ but different entanglement levels (the 41L/174L and 174L/435L series) the relationship between $(G_m'')_L$ and $\phi_L$ is the same even after departure from the $\phi_L^{2.26}$ power law.

Interestingly, $(\omega_m)_L$ appears not to change at all with dilution by S chains. Thus, $\tau_L \equiv (\omega_m)_L^{-1}$ is independent of $\phi_L$, at least over the composition range where an L peak is actually visible. Furthermore, and in contrast with $(G_m'')_L$, the behavior of $\tau_L$ differs fundamentally from that expected if the S component acted like a monomeric diluent. In the latter case, $\tau_L$ would change in the same way as the product $\eta_0 J_e^0$ changes with solvent dilution at constant monomeric friction coefficient.[3] In polybutadiene solutions, $J_e^0 \propto \phi^{-2.24}$,[4] and at constant monomeric friction coefficient, $\eta_0 \propto \phi^{3.4-4.0}$.[2,35,43] Thus, for an isofriction monomeric diluent, $\tau_L$ would vary as $\phi^{1.2-1.8}$, and $(\omega_m)_L$ would shift to higher frequencies no less rapidly than $\phi_L^{-1.2}$. That behavior is shown by the dashed line in Figure 9; the progression of $(\omega_m)_L$ for a well-entangled diluent is observably different.

The shape of the L peak below $(\omega_m)_L$ changes slightly with dilution by S chains. The values of $G''(\omega)$ at $\omega = (\omega_m)_L/10$ fall slightly more rapidly with dilution than $(G_m'')_L$ itself. There may also be an effect of $R$, since these differences only begin to appear for $\phi_L \lesssim 0.56$ for the 41L/435L series ($R = 10.7$), but they are already present at $\phi_L = 0.9$ in the others.

**B. Properties of the S Peak.** Figure 13 shows an expanded plot of $G''(\omega)$ vs. log $\omega$ for the 41L/174L mixtures in the S peak region. At $\phi_L = 0.025$ and 0.05 (not shown) the S peak is virtually unchanged, but at $\phi_L = 0.10$ $(G_m'')_S$ is *higher* while $(\omega_m)_S$ is still unchanged. Then, $(G_m'')_S$ begins a somewhat erratic descent as $\phi_L$ increases further and finally disappears in the growing high-frequency tail of the L peak. Beyond $\phi_L = 0.20$, $(\omega_m)_S$ shifts slowly but persistently to lower frequencies.

We have not attempted a detailed analysis of $(G_m'')_S$. Identification of the part due to S chains would involve an uncertain resolution of peaks to remove the L chain and transition region contributions. The behavior of $(G_m'')_S$ is also not systematic from one series to another. For moderate additions of L chains ($\phi_L \sim 0.1$) the value of $(G_m'')_S$ increases in the 98L/435L solution series as well as 41L/174L (Figure 13), but it remains constant or has already begun to descend in 41L/435L and 174L/435L. The behavior of undiluted 98L/435L appears to be even
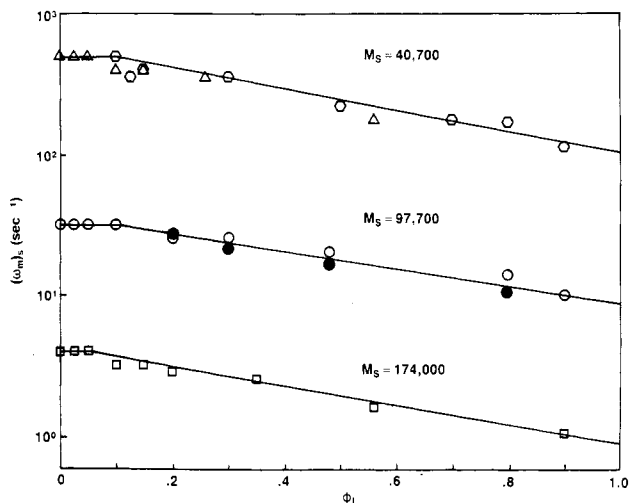
**Figure 14.** Frequency at the loss modulus maximum for the S peak vs. colume fraction of L chains at 25 °C. Symbols indicate the 41L/435L series (▲), the 98L/435L series (○), the 174L/435L series (□), the 41L/174L series (⊙), and the diluted 98L/435L solution series (●).

more anomalous, but those data are suspect for instrumental reasons (see Experimental Section).

For $(\omega_m)_S$, on the other hand, the pattern of behavior is not only systematic but also virtually the same in all the series (Figure 14). Peak separations, governed by $R$ and $M_S/M_e$, vary widely among the series, so the influences of peak overlap are different; nevertheless the shifts in $(\omega_m)_S$ with $\phi_L$ are similar. Also these data for the various undiluted samples were gathered near $|G^*(\omega)| \sim 10^7$ dyn/cm$^2$, so instrumental effects might be a problem (see Experimental Section). However, the relationship between $(\omega_m)_S$ and $\phi_L$ is the same for the solution series, and in this case the moduli near $(\omega_m)_S$ are much smaller.

A short extrapolation in Figure 14 gives $(\omega_m)_S$ at $\phi_L = 1$, which we interpret to be the reciprocal of an average relaxation time for isolated S chains in a matrix of the L chains. Accordingly, $\tau_S \equiv (\omega_m)_S^{-1}$ shifts from its pure component value (an S-chain matrix) to a somewhat larger value in a matrix of longer chains. From Figure 14, the shift factor is 4.8 for sample 41L in either a 174L matrix ($R = 4.3$) or a 435L matrix ($R = 10.7$). The shift factor is 3.7 for 98L in a 435L matrix, either undiluted or diluted 50% by Flexon 391 ($R = 4.5$), and 4.5 for 174L in a 435L matrix ($R = 2.5$). Similar shifts of $\tau_S$ with composition have been noted recently for polystyrene mixtures.[21]

The results here parallel closely the observations of Ferry and co-workers on the relaxation of linear polybutadiene chains dilutely dispersed in a polybutadiene network.[44] Relaxation times in that case, corresponding to $\phi_L \sim 1$ and $R = \infty$, were reported to be larger than the self-matrix values ($\phi_L = 0$) by about half an order of magnitude, i.e., by roughly a factor of 3.

The relaxation time of entangled linear chains in a matrix of longer chains is evidently larger than the pure component value. For polybutadiene the ratio of times is approximately 4 and, within the accuracy of the data, independent of both $M_S$ and $M_L$ for values of $R$ as small as 2.5. The ratio must of course return finally to unity at the self-matrix limit of $R = 1$.

**C. Comments.** The behavior of $(\omega_m)_L$ implies that the relaxation time of chains in mixtures with shorter but still well-entangled chains ($M_S/M_e \gg 1$) is independent of mixture composition. That conclusion is valid here ($M_S/M_e \geqslant 20$) for $R$ as large as 10.7 and for L-chain concentrations as small as $\phi_L \sim 0.25$. It does not apply for
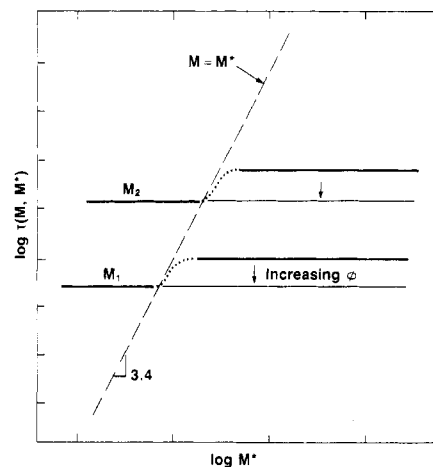


**Figure 15.** Schematic representation of relaxation time vs. matrix molecular weight for highly entangled linear chains. The matrix molecular weight is $M^*$; $M_1$ and $M_2$ are molecular weights for two sizes of relaxing chains.

dilution by oligomers ($M < M_c$) or isofriction monomeric solvents, and it is contrary to observations on entangled polystyrene mixtures where $(\omega_m)_L$ shifts similarly to monomeric dilution.[11,14,17,20,21] The behavior of $(\omega_m)_S$, on the other hand, implies that the relaxation time is increased by a matrix of longer chains. The shift in that case depends only on $\phi_L$, reaching a value of approximately 4 ($R \geqslant 2.5$) for dilutely dispersed short chains ($\phi_L \to 1$).

These observations on highly entangled mixtures are summarized in Figure 15 in terms of $\tau(M,M^*)$, the terminal relaxation time for chains of molecular weight $M$ (concentration $\phi$) in a matrix of molecular weight $M^*$. For $M^* < M$, $\tau(M,M^*)$ shows L-chain behavior, remaining constant at the homologous liquid value, $\tau(M,M)$ at $\phi = 1$, down to concentrations as low as $\phi = 0.25$ and possibly beyond. For $M^* > 2.5M$, $\tau(M,M^*)$ shows S-chain behavior, increasing with dilution by matrix from $\tau(M,M)$ to about 4 times that value at its dilute limit, $\phi = 0$. The crossover occurs somewhere between $M^* = M$ and $M^* = 2.5M$.

The behavior of $(G_m'')_L$ implies that the weighting factor for the terminal relaxation is roughly quadratic in concentration (actually $\phi^{2.26}$, and applying at the left of the $M = M^*$ line in Figure 15). Prest[24] drew a similar conclusion from his polystyrene data and also found the S-chain weighting factor to be linear in $\phi_S$. Our somewhat erratic results for $(G_m'')_S$ are not inconsistent with the Prest proposal; if we accept it, the weighting factor is $\phi$ for $M < M^*$ (on the right of the $M = M^*$ line in Figure 15).

Masuda et al.[26] have recently suggested a mixing law that includes both these features as well as a cross term:

$$H(\tau) = \phi_L^2 H_{LL}(\tau) + \phi_L\phi_S H_{LS}(\tau) + \phi_S H_{SS}(\tau) \quad (19)$$

where the subscripts denote spectra they associated with pairwise L–L, L–S, and S–S interactions. Watanabe et al.[21] have used this form to interpret data on entangled polystyrene mixtures in terms of reptation[28] and tube renewal[36–38] contributions to relaxation. We offer below a slightly different interpretation, but based on the same idea.

According to the tube model[28] the individual components in an entangled mixture contribute to stress in proportion to their volume (or weight) fractions. Thus, for a two-component system in the terminal region

$$G(t) = \phi_L G_L(t/T_L) + \phi_S G_S(t/T_S) \quad (20)$$

where $T_L$ and $T_S$ are reptation (tube disengagement) times. The partial moduli, $G_L(t/T_L)$ and $G_S(t/T_S)$, are identical in form and apply at all concentrations if the tubes are
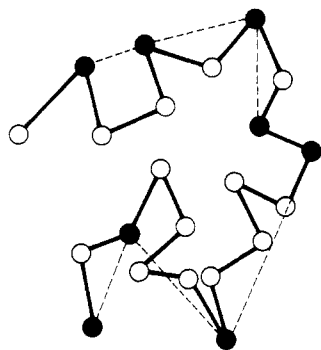
**Figure 16.** Schematic representation of the primitive path for an L chain in a binary mixture. The filled circles represent constraints supplied by other L chains; the open circles are those supplied by other L chains; the open circles are those supplied by S chains. The dashed line is the path defined by L constraints alone.

permanent, i.e., if the constraints that define the tubes have lifetimes much longer than both $T_L$ and $T_S$. In highly entangled liquids $(M_L, M_S \gg M_e)$ the constraints are supplied by neighboring chains which are also reptating. The assumption of tube permanence improves for S chains when diluted by L chains, but it worsens for L chains when diluted by S chains. Thus, we expect $G_L(t/T_L)$ in particular to change with the composition of the mixture. If $T_S \ll T_L$, the relaxation of L chains will occur in two stages.

A qualitative discussion of the effects of constraint release is given here.[52] A quantitative theory will be published elsewhere.[39] Figure 16 depicts the primitive path of an L chain, comprising a large number $N_L$ of independently directed steps, each of length $a$.[25] We assume for simplicity that each junction of steps is localized by one constraint, supplied by either an S chain (fraction $\phi_S$ with lifetime $\sim T_S$) or an L chain (fraction $\phi_L$ with lifetime $\sim T_L$). We treat the L constraints as effectively permanent and assume that the path configuration between them obeys Orwoll–Stockmayer dynamics[38,45] with hop frequency $\sim T_S^{-1}$ and hop distance $\sim a$.

Up to a time of order $T_S$ the path configuration is frozen. Beyond $T_S$ the path configurations between successive L junctions relax by random hopping: $G_L(t/T_L)$ decreases rapidly and then more slowly beyond $T_S$, eventually reaching $t^{-1/2}$ (Rouse-like) behavior if $\phi_L$ is small (many steps between L junctions). That part of the relaxation will cease when the path configurations between L junctions reach equilibrium, and the fraction of $G_L(t/T_L)$ remaining will be $\phi_L$, i.e., the fraction of unrelaxed junctions. This leads directly to a weighting factor proportional to $\phi_L^2$ for the final relaxation according to eq 20.[46] The shape and final relaxation time for the remaining portion of $G_L(t/T_L)$ depends on how the disengagement time is affected by constraint release.

During time intervals of order $T_S$ the directions of all steps in the path are fixed. The time for an L chain to diffuse one step distance along its path is approximately $T_L/N_L^2$. If $T_L/N_L^2 \ll T_S$, the diffusion distance for disengagement is equal to the path length $aN_L$, even though the directions of individual steps of the path may change many times during the full course of disengagement. For this case the final relaxation time is $T_L$ and is independent of $\phi_S$ and $N_S$. On the other hand, if $T_L/N_L^2 \gg T_S$, the S chains do not constrain the local diffusion directions during movements from one junction to the next. The diffusion distance is shorter because only L junctions are involved (Figure 16). There are now $\phi_L N_L$ steps of length $a/\phi_L^{1/2}$, giving a disengagement time in this case of $(aN_L\phi_L^{1/2}/ aN_L)^2 T_L = \phi_L T_L$. Thus, the relaxation time for L chains
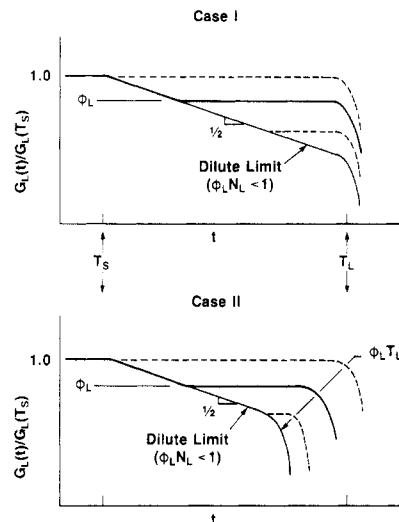


**Figure 17.** Schematic representation of the partial modulus for the long chains in entangled binary mixtures. Case I corresponds to $M_L M_e^2/M_S^3 \leq 0.1$; case II corresponds to $M_L M_e^2/M_S^3 \geq 0.1$.

**Table V**
**Comparison of Constraint Release Parameter for Entangled Mixtures**

| series | $R$ | $M_S/M_e$ | $M_L N_e^2/M_S^3$ | source |
|---|---|---|---|---|
| *Undiluted Polybutadiene ($M_e$ = 1850)* | | | | |
| 174L/435L | 2.5 | 94 | $2.8 \times 10^{-4}$ | this work |
| 41L/174L | 4.3 | 22 | $8.8 \times 10^{-3}$ | this work |
| 98L/435L | 4.5 | 53 | $1.6 \times 10^{-3}$ | this work |
| 41L/435L | 10.7 | 22 | $2.2 \times 10^{-2}$ | this work |
| *Diluted Polybutadiene ($M_e$ = 4400)* | | | | |
| 98L/435L | 4.5 | 22 | $9.0 \times 10^{-3}$ | this work |
| *Undiluted Polystyrene ($M_e$ = 18 000)* | | | | |
| 125L/267L | 2.1 | 7 | $4.4 \times 10^{-2}$ | Akovali[10] |
| 97L/411L | 4.2 | 5.5 | $1.5 \times 10^{-1}$ | Prest and Porter[14] |
| 160L/670L | 4.2 | 9 | $5.3 \times 10^{-2}$ | Marin et al.[18] |
| 87L/500L | 5.8 | 5 | $3.6 \times 10^{-1}$ | Mills and Nevin[13] |
| 161L/294L | 1.8 | 9 | $2.3 \times 10^{-2}$ | Watanabe et al.[21] |
| 83L/294L | 3.5 | 4.5 | $1.7 \times 10^{-1}$ | |
| 36L/294L | 8.2 | 2 | $2.0 \times 10^{0}$ | |
| 36L/407L | 11.3 | 2 | $2.8 \times 10^{0}$ | |
| 100L/2700L | 27 | 5.5 | $8.0 \times 10^{-1}$ | Montfort et al.[20] |

decreases with decreasing $\phi_L$. The latter behavior is also predicted for mixtures by Marrucci's expanding-tube model[46] and is the result expected for dilution by an iso-friction monomeric solvent.

These conclusions are summarized in Figure 17. The dilute limit shown there for each case is reached when $N_L < \phi_L^{-1}$. For case I $(T_L/N_L^2 \ll T_S)$, the longest relaxation time at the dilute limit is $T_L$; for case II $(T_L/N_L^2 \gg T_S)$, the longest relaxation time at the dilute limit is $\sim T_S N_L^2$.

For pure reptation, $T_L/T_S = (M_L/M_S)^3$ and $N_L \sim M_L/M_e$. Thus, from $G^*(\omega)$ measurements on well-entangled binary mixtures we expect

$$(\omega_m)_L = (\omega_m)_L^\circ \qquad \text{(case I)} \qquad (21a)$$

for all $\phi_L$ and $M_S$ when $M_L M_e^2/M_S^3 \ll 1$, and

$$(\omega_m)_L = (\omega_m)_L^\circ \phi_L^{-1} \qquad \text{(case II)} \qquad (21b)$$

for all $M_s$ and $N_L > \phi_L^{-1}$ when $M_L M_e^2/M_S^3 \gg 1$. The same criterion was proposed earlier by Daoud and de Gennes[37] for the absence (case I) or presence (case II) of constraint release (tube renewal) effects on diffusion coefficients. Recent measurements by Kramer and co-workers[47] on tracer diffusion in various polystyrene matrices suggest that the crossover occurs near $M_L M_e^2/M_S^3 = 0.1$. Values
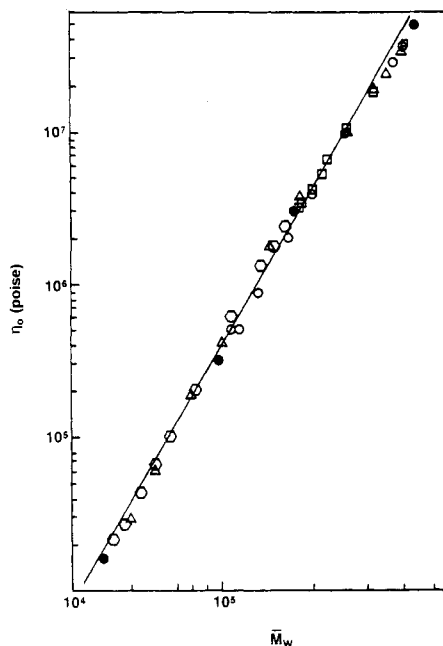
**Figure 18.** Viscosity vs. weight-average molecular weight for binary mixtures of polybutadiene at 25 °C. Pure component values are indicated by filled symbols. The solid line is eq 15.
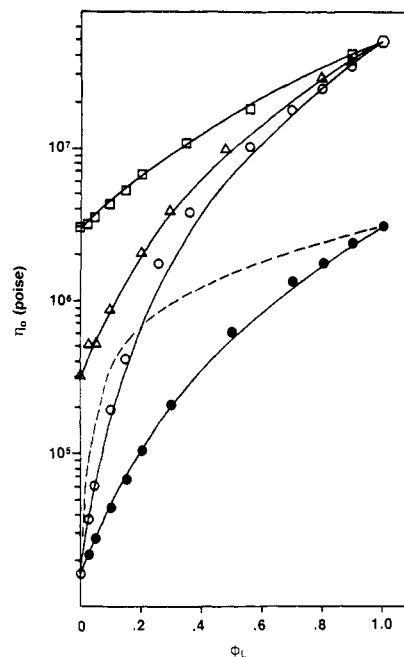


**Figure 19.** Viscosity vs. volume fraction of long chains in binary mixtures of undiluted polybutadiene at 25 °C. Symbols indicate data for the 41L/435L series (O), the 174L/435L series (□), the 98L/435L series (△), and the 41L0174 series (◻). The solid lines were calculated from eq 22 with $\alpha = 3.41$.

for the polybutadiene mixtures used here and for several polystyrene mixtures used in studies of viscoelastic behavior are given in Table V. The polybutadiene mixtures clearly belong in the case I category. The values of $M_{\mathrm{L}}M_{\mathrm{e}}^2/M_{\mathrm{S}}^3$ are much larger for the polystyrene mixtures and generally fall in the case II category ($M_{\mathrm{L}}M_{\mathrm{e}}^2/M_{\mathrm{S}}^3 > 0.1$) when $R$ is large enough to provide a relatively clear picture of $(\omega_{\mathrm{m}})_{\mathrm{L}}$ behavior. This seems, therefore, to account satisfactorily for the observed differences between polybutadiene and polystyrene in $(\omega_{\mathrm{m}})_{\mathrm{L}}$ dependence on $\phi_{\mathrm{L}}$.

There still remains, however, the question of why $\tau$-$(M,M^*)$ shifts in magnitude near $M = M^*$ (Figure 15) even though matrix effects on the relaxation time are supposed to be negligible in our case I mixtures. We believe that shift merely reflects a change in relaxation spectrum *shape* from the pure reptation form for $M \leqslant M^*/2.5$ and small $\phi$ to the reptation–constraint release form otherwise. The definition $\tau \equiv (\omega_{\mathrm{m}})^{-1}$ is quite arbitrary, of course, and, considering that the weighting factor for the peak changes from $\phi^2$ to $\phi$ near $M = M^*$, a corresponding shift in peak shape is not surprising. Furthermore, the increase in $\tau$-$(M,M^*)$ with decreasing $\phi$ for $M < M^*$ should be viewed as an influence of changing spectral shape with decreasing constraint release contributions, not as a shift in relaxation time, per se.

**2. Viscosity.** The viscosity $\eta_0$ is shown as a function of weight-average molecular weight $\bar{M}_{\mathrm{w}}$ in Figure 18 for the four undiluted series. Values of $\bar{M}_{\mathrm{w}}$ were calculated from $\phi$ and the component molecular weights with eq 12. The line is eq 15, the pure component relationship for polybutadiene, and data for the mixtures fall nicely along that line. The departures are small and seem mainly related to deviations of the pure component values for eq 15, perhaps due to small inaccuracies in the molecular weights. That uncertainty can be eliminated by expressing the weight-average dependence in terms of pure components viscosities.[17] From eq 11 and 12

$$\eta_0 = [\phi_{\mathrm{S}}(\eta_0)_{\mathrm{S}}^{1/\alpha} + \phi_{\mathrm{L}}(\eta_0)_{\mathrm{L}}^{1/\alpha}]^\alpha \qquad (22)$$

Viscosities from Figure 18 are replotted in Figure 19 as a function of $\phi_{\mathrm{L}}$. The solid lines were calculated from eq 22 with $\alpha = 3.41$ from eq 15. Midrange departures which

increase with $R$ are visible but clearly small even at $R = 10.7$.

Other forms of dependence on polydispersity have been proposed. According to Malkin et al.[15]

$$\eta_0 = K(\bar{M}_{\mathrm{w}})^{3.4}(\bar{M}_z/\bar{M}_{\mathrm{w}})^{1.5} \qquad (23)$$

which closely resembles an early prediction by Bueche.[48] From the Doi–Edwards theory,[28,49] adjusted to give the observed pure component behavior (eq 15),

$$\eta_0 = K(\bar{M}_{\mathrm{w}}\bar{M}_z\bar{M}_{z+1})^{3.41/3.0} \qquad (24)$$

These expressions can be recast in terms of moments of the weight distribution function

$$Q_j = \sum_i M_i^j \phi_i \qquad (25)$$

and for two-component mixtures

$$Q_j = M_{\mathrm{S}}^j[1 + (R^j - 1)\phi_{\mathrm{L}}] \qquad (26)$$

If eq 23 is correct, the expression for $\eta_0$ in eq 22 should be multiplied by $(Q_2/Q_1{}^2)^{1.5}$, and if eq 24 is correct, the expression for $\eta_0$ in eq 22 should be multiplied by $(Q_3/Q_1{}^3)^{3.41/3}$. The result for eq 24 for the 41L/174L series is shown by the dashed line in Figure 19. Departures from the unmodified eq 22 are clearly much smaller.

The largest departures from eq 22 occur for the 41L/435L series ($R = 10.7$) near $\phi_{\mathrm{L}} = 0.2$–0.3. At $\phi_{\mathrm{L}} = 0.26$, the experimental value is $\eta_0 = 1.75 \times 10^6$ P (Table IV). Equation 24 gives $12.5 \times 10^6$ P, eq 23 gives $3.9 \times 10^6$ P, and eq 23 with $(\bar{M}_z/\bar{M}_{\mathrm{w}})^{1.5}$ replaced by $\bar{M}_{\mathrm{n}}/\bar{M}_{\mathrm{w}}$ (eq 23b in ref 30) gives $0.23 \times 10^6$ P. None of these provides an improvement on the simple weight-average law (eq 22), which gives $\eta_0 = 1.07 \times 10^6$ P, about 40% smaller than the experimental value.

Figure 20 shows $\eta_0$ vs. $\bar{M}_{\mathrm{w}}$ for the diluted and undiluted 98L/435L series. The lines are parallel; the average ratio of viscosities (diluted/undiluted) at constant $\bar{M}_{\mathrm{w}}$ is 0.22. The free volume correction for the viscosity of polybutadiene in Flexon 391 (volume fraction of polymer $\phi_{\mathrm{p}}$
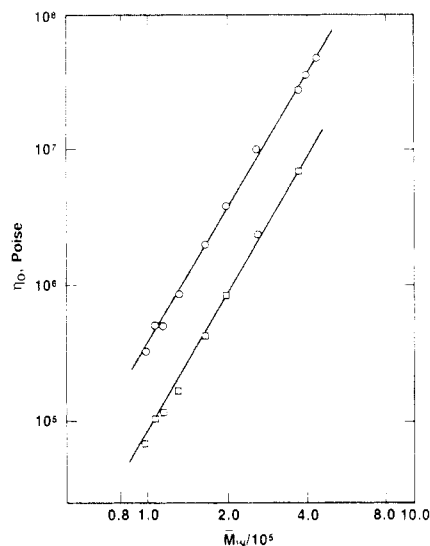
**Figure 20.** Viscosity vs. weight-average molecular weight for the diluted and undiluted 98L/435L and solution series of binary mixtures at 25 °C. Symbols indicate the undiluted mixtures (O) and 50 wt % solutions in Flexon 391 (□).

= 0.52) is 0.508 at 25 °C.[18,26] The ratio of viscosities at constant $\bar{M}_w$ and constant monomeric friction coefficient is therefore (0.22)(0.508) = 0.112. That value agrees well with a 3.41 power dependence on concentration, $(0.52)^{3.41}$ = 0.108 and is different from the 4.0 power law reported earlier,[18] $(0.53)^4$ = 0.073. The viscosity data for diluted and undiluted 98L/435L series, corrected to constant monomeric friction, would superimpose accurately if plotted as a function of $\phi_p \bar{M}_w$.

In summary, the "weight-average" law for viscosity (eq 11) works very well indeed for entangled binary mixtures, as many previous workers have found.[2,9,14,17,33,50] That relationship goes over directly to $\eta_0 = K(\phi_L M_L)^\alpha$ for $R \to \infty$, which is also the behavior for dilution by isofriction monomeric solvents,[2] as we have shown here as well.

**3. Recoverable Compliance.** The relationship between $J_e°$ and $\phi_L$ for the four undiluted series is shown in Figure 21. As expected, $J_e°$ passes through a prominent maximum, $(J_e°)_{max}$ at $(\phi_L)_{max}$. As $R$ increases, $(J_e°)_{max}$ rises rapidly and $(\phi_L)_{max}$ moves to lower values. Interestingly, $(\phi_L)_{max}$ changes with $R$ in such a way that $(\bar{M}_w)_{max}/M_S = 1 + (R - 1)\phi_{max}$ is nearly a constant, $(\bar{M}_w)_{max}/M_S \sim 1.35$, over the observed range, $2.5 \leq R \leq 10.7$.

For the data here, $J_e°/(J_e°)_S$ vs. $\phi_L$ is a function of $R$ alone. Within experimental error, $J_e°(\phi_L)$ coincides for the 98L/435L ($R$ = 4.5) and 41L/174L ($R$ = 4.3) series, and $J_e°(\text{soln})/J_e°(\text{melt})$ is practically independent of composition for the diluted and undiluted 98L/435L series (Table 4e). Thus, the reduced compliance $J_e°/(J_e°)_S$, expressed as either a function of $\phi_L$ or $\bar{M}_w/M_S$, is independent of both entanglement spacing $M_e$ and distance from the entanglement threshold $M_S/M_e$.

The line in Figure 21 corresponds to $J_e° \equiv \phi_L^{-2.24}$, the relationship for entangled polybutadienes in monomeric solvents and polybutadiene oligomers ($M < M_c$).[4] All four series approach this behavior at high $\phi_L$, and, as in the case of $(G_m'')_L$ (Figure 12), the agreement with the monomeric dilution law persists to smaller $\phi_L$ as $R$ increases, reaching as low as $\phi_L \sim 0.2$ for $R$ = 10.7 (the 41L/435L series).

Various relationships between $J_e°$ and polydispersity have been proposed. They take the form[3]

$$J_e° = (J_e°)^{\ddagger}P \tag{27}$$

where $(J_e°)^{\ddagger}$ is the pure component value (equal to either
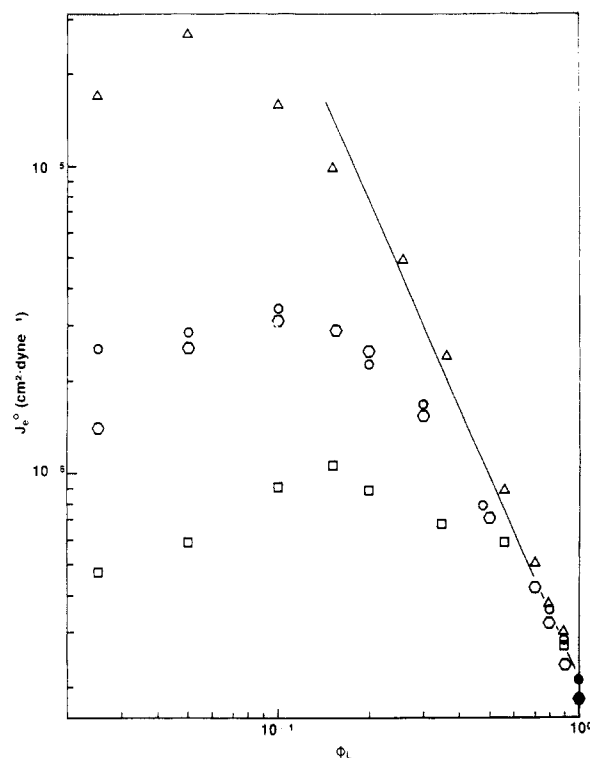


**Figure 21.** Recoverable compliance vs. volume fraction of the long chains for the undiluted binary mixtures. The symbols denote data for the 174L/435L series (△), the 98L/435L series (O), the 174/435L series (□), and the 41L/174L series (O). The line (slope = -2.24) represents the behavior of entangled polybutadienes diluted by monomeric solvents and oligomeric polybutadiene.
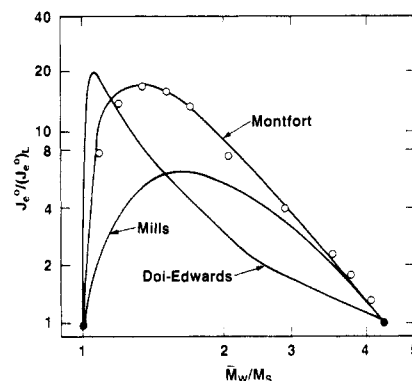


**Figure 22.** Reduced compliance vs. weight-average molecular weight for mixtures in the 41L/174L series. The curves are calculated from the polydispersity factors according to Doi and Edwards (eq 30), Montfort (eq 31), and Mills (eq 28).

$(J_e°)_S$ or $(J_e°)_L$ for $M$ beyond $M_c'$) and $P$ is the polydispersity factor. Mills[32] has suggested

$$P = (\bar{M}_z/\bar{M}_w)^{3.7} = (Q_2/Q_1^2)^{3.7} \tag{28}$$

and for the modified Rouse model[2,3]

$$P = \bar{M}_z\bar{M}_{z+1}/\bar{M}_w^2 = Q_3/Q_1^3 \tag{29}$$

According to the Doi–Edwards theory[28,49]

$$P = Q_6/Q_3^2 \tag{30}$$

and from Montfort et al.,[17] for a viscosity exponent of 3.4 and $(J_e°)_S = (J_e°)_L$,

$$P = Q_{4.4}/Q_1^{4.4} \tag{31}$$

Agarwal[34] has suggested

$$P = \bar{M}_z\bar{M}_{z+1}/\bar{M}_n\bar{M}_w = Q_3Q_{-1}/Q_1^2 \tag{32}$$

and other forms have been considered as well.[21,23,25,27,29,30]

### Table VI
### Properties of the Recoverable Compliance Peak in Binary Mixtures

| series | $R$ | $M_S/M_e$ | $\phi_{max}$ | $(\bar{M}_w/M_S)_{max}$ | $(J_e^\circ)_{max}/(J_e^\circ)_S$ | source |
|---|---|---|---|---|---|---|
| | | | Polybutadiene | | | |
| 174L/435L | 2.5 | 98 | ~0.15 | ~1.25 | 5.4 | this work |
| 41L/174 | 4.3 | 31 | ~0.10 | ~1.35 | 16 | this work |
| 98L/435L | 4.5 | 50 | ~0.10 | ~1.35 | 17 | this work |
| 98L/435L(soln) | 4.5 | 21 | ~0.10 | ~1.35 | 17 | this work |
| 41L/435L | 10.7 | 21 | ~0.05 | ~1.5 | 160 | this work |
| | | | Polystyrene | | | |
| 125L/267L | 2.1 | 7 | ~0.30 | ~0.35 | 1.9 | Akovali[10] |
| 97L/411L | 4.2 | 5.5 | ~0.10 | ~1.3 | 9 | Prest and Porter[14] |
| 160L/670L | 4.2 | 9 | ~0.15 | ~1.5 | 10 | Marin et al.[18] |
| 87L/500 | 5.8 | 5 | ~0.15 | ~11.7 | 20 | Mills and Nevin[13] |
| 100L/2700L | 27 | 5.5 | ~0.05 | ~2.3 | ~300 | Montfort et al.[20] |
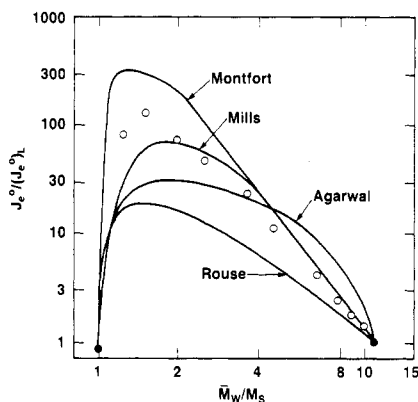


**Figure 23.** Reduced recoverable compliance vs. weight-average molecular weight for mixtures in the 41L/435L series. The curves were calculated from the polydispersity factors according to Agarwal (eq 32), Rouse (eq 29), Mills (eq 28), and Montfort (eq 31).

Comparisons with some of these proposals are shown in Figure 22 (the 41L/174L results, $R$ = 4.5) and Figure 23 (the 41L/435L results, $R$ = 10.7).

The Doi–Edwards form does not agree with the data at $R$ = 4.5 (Figure 22) and the disagreement is even more pronounced for larger $R$. The Mills expression gives reasonable agreement for $R$ = 10.7 (Figure 23) but predicts values which are too small for $R$ = 4.5 (Figure 22). Expressions which involve smaller powers of $\bar{M}_z/\bar{M}_w$[23,25] must of course be even less satisfactory in this regard. The Montfort form gives remarkably good agreement for $R$ = 4.5 (Figure 22). Although predicting a maximum that is somewhat too large for $R$ = 10.7 (Figure 23), eq 31 nevertheless locates the maximum at $\bar{M}_w/M_s \sim 1.27$ for $R \geq 2.5$, which is close to the observed result (Table VI) and a property not given by the other forms. The Agarwal and Rouse expressions predicts a maximum which is much too small at $R$ = 10.7 (Figure 23).

We have not examined exhaustively the various suggested expressions for $P$. The forms tested above were selected on the basis of simplicity and absence of arbitrary parameters. Of these, the form suggested by Montfort et al.[17] is by far the most satisfactory for our data. The molecular basis of the assumed mixing law is by no means evident however.

Estimates of $(J_e^\circ)_{max}/(J_e^\circ)_L$, $\phi_{max}$, and $(\bar{M}_w)_{max}/M_S$ are given in Table VI for literature data on polystyrene mixtures where both components are entangled. As in mixtures of polybutadiene, $(J_e^\circ)_{max}/(J_e^\circ)_L$ increases rapidly with $R$, going roughly as $R^2$ or slightly stronger, and $(\phi_L)_{max}$ drifts to smaller values such that $(\bar{M}_w)_{max}/M_S$ remains nearly constant. The results in Figure 24 show that $(J_e^\circ)_{max}/(J_e^\circ)_L$ is slightly smaller at each $R$ for the polystyrene mixtures. This may be another example of case
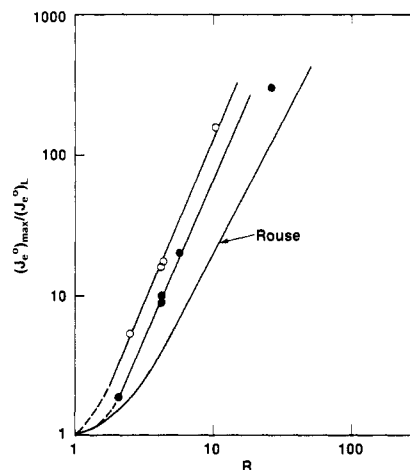


**Figure 24.** Maximum recoverable compliance in binary mixtures as a function of the component molecular weight ratio. The data for polybutadiene mixtures (O) and polystyrene mixtures (●) were taken from Table VI. The Rouse locus was calculated from eq 29.

I vs. case II differences, discussed earlier under Comments. The prediction of the Rouse expression (eq 29), which describes farily well the behavior at relatively low entanglement densities,[2] is shown for comparison. Perhaps the polydispersity dependence moves progressively from Rouse behavior at low entanglement densities, through case II behavior where the L-chain relaxation time is shifted by dilution with S chains, and finally to case I behavior where the presence of S chains does not change $\tau_L$.

It is interesting to compare behavior of $J_e^\circ$ vs. $\phi_L$ for various values of $R$, when both components are well entangled, with monomeric dilution behavior, corresponding to the nonentangled S-chain limit of $R = \infty$. Figure 25 shows smoothed curves for $M_L$ = 435 000 with shorter chain "diluents" of $M_S$ = 174 000 ($R$ = 2.5), $M_S$ = 97 700 ($R$ = 4.5), and $M_S$ = 40 700 ($R$ = 10.7). The dashed line represents monomeric diluent behavior, which we have constructed as follows.

At high concentrations, $J_e^\circ = 2.1 \times 10^{-7}\phi_L^{-2.24}$,[4] and this persists until a crossover to $\phi_L^{-1}$ Rouse behavior (eq 7 with $c = \rho\phi_L$).[3] For $M$ = 435 000 that crossing occurs at $\phi_L \sim$ 0.05. In the dilute regime, $J_e^\circ \propto \phi_L$, and according to the Zimm model[2]

$$J_e^\circ = 0.205 \frac{M[\eta]_L^2\rho}{RT}\phi_L \tag{33}$$

Ignoring excluded volume effects, which are probably not relevant here anyway, $[\eta]_L = ([\eta]_L)_\Theta = 117$ cm$^3$/g for polybutadiene with $M$ = 435 000,[51] giving $J_e^\circ = 0.044\phi_L$. Intersection with the Rouse line occurs near the overlap concentration $\phi_L^* \sim 1/\rho[\eta]_L$, giving $(J_e^\circ)_{max} \sim 4 \times 10^{-4}$
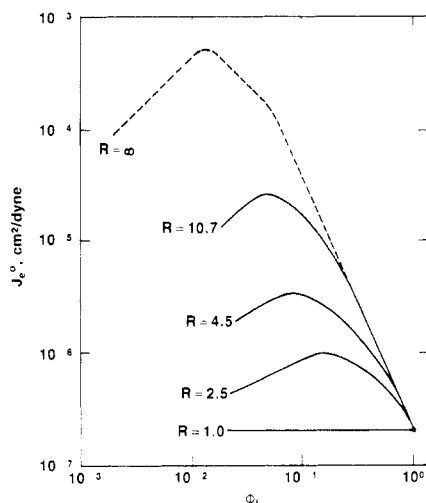
**Figure 25.** Comparison of recoverable compliance for sample 435L diluted by shorter chains and solvents. The solid curves are smoothed data for the 174L/435L series ($R$ = 2.5), the 98L/435L series ($R$ = 4.5), and the 41L/435L series ($R$ = 10.7). The dashed curve is the behavior in a monomeric solvent, constructed as described in the text.

cm$^2$/dyn for a monomeric diluent. In the observable range, the $J_e^\circ$ vs. $\phi_L$ curves for the entangled mixtures are contained nicely within the envelope provided by monodisperse ($R$ = 1) and monomeric diluent ($R$ = ∞) behavior. The dependence approaches the $R$ = ∞ curve rapidly with increasing $R$: $(J_e^\circ)_{max}/(J_e^\circ)_L = (4 \times 10^{-4})/(2 \times 10^{-7}) = 2000$ for a monomeric diluent, and that ratio is already 160 at $R$ = 10.7 and rising rapidly. From an extrapolation based on Figure 24, $(J_e^\circ)_{max}/(J_e^\circ)_L$ would reach 2000 at $R \sim 30$, corresponding to $M_S \sim 435000/30 = 14500$. It is possible that the monomeric dilution curve for a polymer represents an upper bound on $J_e^\circ$ vs. $\phi_L$ for all its mixtures with smaller species, but that it still not known.

## Summary and Conclusions

Dynamic moduli in the plateau and terminal regions were measured for binary mixtures of linear polybutadiene. Relaxation times and weighting factors for the individual components were obtained from the L (long chain) and S (short chain) peaks in the loss modulus. These varied systematically with mixture composition and accorded well with expectations based on reptation and constraint release ideas. Differences between these results and data on entangled polystyrene mixtures appear to be related to the magnitude of $M_L M_e^2/M_S^3$, a parameter which governs the effect of constraint release on the relaxation time of the L-chain component. Viscosity and recoverable compliance varied systematically with mixture composition, $\eta_0$ governed primarily by $\bar{M}_w$ for the mixture, and $J_e^\circ$ passing through an increasingly prominent maximum at intermediate compositions with increasing $M_L/M_S$. Several proposed mixing laws were compared with the data on $\eta_0$ and $J_e^\circ$. The Montfort proposal was the most successful, but none of those with a molecular basis could be considered adequate.

## References and Notes

(1) (a) Current address: Exxon Chemical Co., Linden, NJ 07036. (b) Current address: Corporate Research Laboratories, Exxon Research and Engineering Co., Annandale, NJ 08801.
(2) Ferry, J. D. "Viscoelastic Properties of Polymers", 3rd ed.; Wiley: New York, 1980.
(3) Graessley, W. W. *Adv. Polym. Sci.* **1974**, *16*, 1.
(4) Raju, V. R.; Menezes, E. V.; Marin, G.; Graessley, W. W.; Fetters, L. J. *Macromolecules* **1981**, *14*, 1668.
(5) Gotro, J. T.; Graessley, W. W. *Macromolecules* **1984**, *17*, 2767.
(6) Carella, J. M.; Fetters, L. J.; Graessley, W. W.; *Macromolecules* **1984**, *17*, 2775.
(7) Graessley, W. W.; Edwards, S. F. *Polymer* **1981**, *22*, 1329.
(8) Leaderman, H.; Smith, R. G.; Williams, L. C. *J. Polym. Sci.* **1959**, *36*, 233.
(9) Ninomiya, K.; Ferry, J. D. *J. Phys. Chem.* **1963**, *67*, 2297.
(10) Akovali, A. *J. Polym. Sci., Part A-2* **1967**, *5*, 875.
(11) Masuda, T.; Kitagawa, K.; Inoue, T.; Onogi, S. *Macromolecules* **1970**, *3*, 116.
(12) Onogi, S.; Masuda, T.; Toda, N.; Koga, K. *Polym. J.* **1970**, *1*, 542.
(13) Mills, N. J.; Nevin, A. *J. Polym. Sci., Part A-2* **1971**, *9*, 267.
(14) Prest, W. M.; Porter, R. S. *Polym. J.* **1973**, *4*, 154.
(15) Malkin, A. Y., et al. *Eur. Polym. J.* **1974**, *10*, 445.
(16) Yanovskii, Yu. G.; Vinogradov, G. V.; Ivanova, L. I. *Polym. Sci. USSR (Engl. Transl.)* **1982**, *24*, 1194 (*Vysokomol. Soedin., Ser. A* **1982**, *24*, 1057).
(17) Montfort, J. P.; Marin, G.; Arman, J.; Monge, Ph. *Polymer* **1978**, *19*, 277.
(18) Marin, G.; Montfort, J. P.; Arman, J.; Monge, Ph. *Rheol. Acta* **1979**, *18*, 629.
(19) Schausberger, A.; Schindlauer, G.; Janeschitz-Kriegl, H. *Rheol. Acta* **1983**, *22*, 550.
(20) Montfort, J. P.; Marin, G.; Monge, P. *Macromolecules* **1984**, *17*, 1551.
(21) Watanabe, H.; Kotaka, T. *Macromolecules* **1984**, *17*, 2316. Watanabe, H.; Sakamoto, T.; Kotaka, T. *Macromolecules* **1984**, *18*, 1008.
(22) Ninomiya, K.; Ferry, J. D. *J. Colloid Sci.* **1963**, *18*, 421.
(23) Bogue, D. C.; Masuda, T.; Einaga, Y.; Onogi, S. *Polym. J.* **1970**, *1*, 563.
(24) Prest, W. M. *Polym. J.* **1971**, *4*, 163.
(25) Kurata, M.; Osaki, K.; Einaga, Y.; Sugie, T. *J. Polym. Sci., Polym. Phys. Ed.* **1974**, *12*, 849.
(26) Masuda, T.; Yoshimatsu, S.; Takahashi, M.; Onogi, S. *Polym. Prepr. Jpn.* **1983**, *32*, 2365.
(27) Graessley, W. W. *J. Chem. Phys.* **1971**, *54*, 5143.
(28) Doi, M.; Edwards, S. F. *J. Chem. Soc., Faraday Trans. 2*, **1978**, *74*, 1789; **1978**, *74*, 1802.
(29) Liu, T. Y.; Soong, D.; Williams, M. *J. Rheol.* **1983**, *27*, 7 and previous papers referenced therein.
(30) Kurata, M. *Macromolecules* **1984**, *17*, 895.
(31) Graessley, W. W. *Faraday Soc. Symp.* **1983**, *18*, 7.
(32) Mills, N. J. *Eur. Polym. J.* **1969**, *5*, 675.
(33) Friedman, E. M.; Porter, R. S. *Trans. Soc. Rheol.* **1975**, *19*, 493.
(34) Agarwal, P. K. *Macromolecules* **1979**, *12*, 343.
(35) Marin, G.; Menezes, E. V.; Raju, V. R.; Graessley, W. W. *Rheol. Acta* **1980**, *19*, 462.
(36) Klein, J. *Macromolecules* **1978**, *11*, 852.
(37) Daoud, M.; de Gennes, P.-G. *J. Polym. Sci., Polym. Phys. Ed.* **1979**, *17*, 1971.
(38) Graessley, W. W. *Adv. Polym. Sci.* **1982**, *47*, 67.
(39) Helfand, E.; Rubinstein, M.; Graessley, W. W.; Pearson, D. S., manuscript in preparation.
(40) Struglinski, M. J. Doctoral Thesis, Northwestern University, 1984.
(41) Rochefort, W. E.; Smith, G. G.; Rachapudy, H.; Raju, V. R.; Graessley, W. W. *J. Polym. Sci., Polym. Phys. Ed.* **1979**, *17*, 1197.
(42) Zhongde, X.; Mingshi, S.; Hadjichristidis, N.; Fetters, L. J. *Macromolecules* **1981**, *14*, 1591.
(43) Colby, R. H., M.S. Thesis, Chemical Engineering Department, Northwestern University, 1983.
(44) Kan, H.-C.; Ferry, J. D.; Fetters, L. J. *Macromolecules* **1980**, *13*, 1571.
(45) Orwoll, R. A.; Stockmayer, W. H. *Adv. Chem. Phys.* **1969**, *15*, 305.
(46) Marrucci, G. *J. Polym. Sci., Polym. Phys. Ed.* **1985**, *23*, 159.

(47) Green, P. F.; Mills, P. J.; Palmstrom, C. J.; Mayer, J. W.; Kramer, E. J. *Phys. Rev. Lett.* **1984**, *53*, 2145.
(48) Beuche, F. "Physical Properties of Polymers"; Interscience: New York, 1962.
(49) Graessley, W. W. *J. Polym. Sci., Polym. Phys. Ed.* **1980**, *18*, 27.
(50) Fox, T. G.; Berry, G. C. *Adv. Polym. Sci.* **1968**, *5*, 261.

(51) Hadjichristidis, N.; Zhongde, X.; Fetters, L. J.; Roovers, J. *J. Polym. Sci., Polym. Phys. Ed.* **1982**, *20*, 743.
(52) Our interpretation of the weighting factor and relaxation time for L chains owe much to a discussion with Y.-H. Lin of Exxon Chemical Co. whose internal report in 1983 clearly anticipated some of the conclusions drawn here.

# Decomposition of Entropy and Enthalpy for the Melting Transition of Polyethylene

## John F. Nagle*

*Departments of Physics and Biological Sciences, Carnegie-Mellon University, Pittsburgh, Pennsylvania 15213*

## Martin Goldstein

*Division of Natural Science and Mathematics, Yeshiva University, New York, New York 10033. Received May 1, 1985*

ABSTRACT: In order to estimate the relative importance of various features to the melting transition of polyethylene it is useful to make estimates, based on as much data as possible, of how much each feature contributes to the entropy change and to the enthalpy change. Most of the enthalpy change (980 cal/mol $CH_2$) is accounted for by a cohesive, van der Waals energy term ($\Delta U_{vdW} \sim 720$ cal/mol) and a rotameric term ($\Delta U_R \sim 200$ cal/mol). The entropy change (2.36 eu) is adequately accounted for by a conformational term ($\Delta S_C \sim 1.7$ eu), an excluded volume term ($\Delta S_X \sim -0.7$ eu), and a volume expansion term ($\Delta S_V \sim 1.3$ eu). In view of the differences between these results and previous results, the statistical mechanical fundamentals of such decompositions are discussed in detail and reasons for rejecting some previous conventions are given. The magnitudes of the volume term $\Delta S_V$ and the cohesive term $\Delta U_{vdW}$ indicate that such interactions and the concomitant volume expansion are major factors in the melting of polyethylene.

## I. Introduction

To being to understand a phase transition it is useful and appropriate to do some simple approximate, phenomenological calculations to evaluate those features that one thinks might play major roles in the transition. One procedure is to identify the different distinct features that might be important and then to study them quantitatively one at a time. In the case of polymer melting such calculations have usually focused on the entropy, which has been decomposed[1-10] as follows:

$$\Delta S_M = \Delta S_C + \Delta S_V \tag{1}$$

In eq 1 $\Delta S_M$ is the measured entropy of melting obtained from the measured enthalpy, $\Delta H_M$, divided by the melting temperature, $T_M$. The first term of the decomposition, $\Delta S_C$, is the increase in conformational entropy of single chains. The second term in the decomposition, $\Delta S_V$, is defined to be the entropy increase that would have occurred if the measured volume increase had occurred without any other kinds of disordering, such as conformational disordering. A more refined decomposition[11-13] that has in fact led to the previous one is

$$\Delta S_M = \Delta S_R + \Delta S_V + \Delta S_D \tag{2}$$

The term, $\Delta S_R$, where the R stands for rotational isomerism, accounts for chain conformational entropy, but it also includes excluded volume effects. The final term, $\Delta S_D$, has been called the disordering entropy. It includes all other effects. It has been associated with the communal entropy[7-10] and it has been called the disordering entropy common to all liquids;[11-13] other possible sources will be mentioned later.

Another decomposition, one that has not received so much attention, focuses on the enthalpy as follows:[14-17]

$$\Delta H_M = \Delta U_R + \Delta U_{vdW} + \Delta U_0 + P\Delta V \tag{3}$$

where each $U_i$ is the internal energy for the *i*th feature in the system, $\Delta U_R$ is the change in trans–gauche rotameric energy, $\Delta U_{vdW}$ is the change in cohesive van der Waals energy due to the volume change, and $\Delta U_0$ is a small error term that includes all other effects. The $P\Delta V$ term is numerically negligible for polymer melting at atmospheric pressure, amounting to less than 0.01% of the total enthalpy[5] of melting in polyethylene ($\Delta H_M = 980$ cal/mol $CH_2$), but this term will be included formally for completeness.

The first reason that decompositions such as the ones in eq 1–3 could be useful is that, if the sum of the decomposed terms adds up to the measured total, then one has some confidence that one knows all the most important features of the transition. The second reason concerns the relative magnitudes of the substituent contributions to $\Delta H_M$ or $\Delta S_M$. These relative magnitudes give some measure of the relative importance of the various features that give rise to them. Of course, in a complete statistical mechanical treatment of a model with several different features, the ensuing transition is really due to all the features. For example, it is possible that two model features may be essential for the transition in the sense that it would not occur at all if either were absent. Another example is that the change in excluded volume interaction, $\Delta U_X$, is by definition zero, so excluded volume interactions play no role in the enthalpy decomposition; nevertheless, no sharp transition would ever occur without them. Therefore, such decompositions, even if performed accurately, should be interpreted cautiously. Nevertheless, if one of the terms in both the entropy and the enthalpy decompositions is small compared with the others, then the corresponding physical feature can often be said to be minor. Then, when one attempts to construct complete statistical mechanical theories, one has some justification in ignoring such minor features so that the model can be